Seasonal Variation of Legacy Organochlorine Pesticides (OCPs) from East Asia to the Arctic Ocean

Hongyuan Zheng[1], Yuan Gao[2], Yinyue Xia[2], Haizhen Yang[1], and Minghong Cai[2]

[1]Tongji University
[2]Polar Research Institute of China

November 24, 2022

Abstract

Large-scale field investigations of 7 legacy organochlorine pesticides (OCPs) in the surface seawater and atmosphere from East Asia to the high Arctic Ocean were completed in 2017 and 2016. Seawater OCPs (SOCPs) concentrations displayed rapid and significant seasonal variations during mid-late summer. The ocean is the most significant atmospheric-OCP source region for the Arctic, and feedback affects the mid or low latitude regions of the Northern Hemisphere. The legacy OCP concentrations in the Arctic Ocean were shown to gradually decrease with distance from water masses originating in the Bering Sea and the landmass of Alaska. This study is the first updated investigation of OCPs along the North Pacific Ocean to the Arctic Ocean transect in the past decade. It provides updated field data on the global fate of OCPs in a region undergoing rapid climate change.

Hosted file

`supportinformation_table.docx` available at https://authorea.com/users/547383/articles/602722-seasonal-variation-of-legacy-organochlorine-pesticides-ocps-from-east-asia-to-the-arctic-ocean

Hosted file

`supportinformation_text.docx` available at https://authorea.com/users/547383/articles/602722-seasonal-variation-of-legacy-organochlorine-pesticides-ocps-from-east-asia-to-the-arctic-ocean

Seasonal Variation of Legacy Organochlorine Pesticides (OCPs) from East Asia to the Arctic Ocean

Hongyuan Zheng[1,2,3], Yuan Gao[1], Yinyue Xia[1], Haizhen Yang[2,3], and Minghong Cai[1]

[1]Ministry of Natural Resources Key Laboratory for Polar Sciences, Polar Research Institute of China, 451 Jinqiao Road, Shanghai 200136, China

[2]College of Environmental Science and Engineering, Tongji University, 1239 Siping Road, Shanghai 200092, China

[3]State Key Laboratory of Pollution Control and Resource Reuse, Tongji University, 1239 Siping Road, Shanghai 200092, China

Correspondence to: M.-H, Cai,

Tel.: +86-21-58717635; fax: +86-21-58711663

E-mail: caiminghong@pric.org.cn

Abstract

Large-scale field investigations of 7 legacy organochlorine pesticides (OCPs) in the surface seawater and atmosphere from East Asia to the high Arctic Ocean were completed in 2017 and 2016. Seawater OCPs (Σ_7OCPs) concentrations displayed rapid and significant seasonal variations during mid-late summer. The ocean is the most significant atmospheric-OCP source region for the Arctic, and feedback affects the mid or low latitude regions of the Northern Hemisphere. The legacy OCP concentrations in the Arctic Ocean were shown to gradually decrease with distance from water masses originating in the Bering Sea and the landmass of Alaska. This study is the first updated investigation of OCPs along the North Pacific Ocean to the Arctic Ocean transect in the past decade. It provides updated field data on the global fate of OCPs in a region undergoing rapid climate change.

Plain Language Summary

We investigated 4 hexachlorocyclohexanes (HCHs) and 3 dichlorodiphenyltri--chloroethanes (DDTs) in the marine boundary and their fate corresponding to the geophysical climate change from East Asia to the high Arctic during 2 Arctic Research Expedition cruises. Levels of OCPs in the surface seawater between the forward and return voyages along the same transect indicated the rapid seasonal variation. The reducing DDT contamination and comparable HCH levels to the previous studies in the low latitude regions indicated the effective control measures in the past decades. However, the potential point source and agriculture activities still resulted in the high levels of DDTs in East Asia. Water mass from the Bering Sea significantly affected the levels of dissolved OCPs in the Arctic Ocean, while China, Japan, and East Russia were the crucial source regions for the atmospheric OCPs in East Asia. The Arctic Ocean becomes a significant source region, and possible feedback affects the low latitude regions in East Asia.

Key Points:

- OCPs displayed a significant seasonal variation in the surface seawater;

- The Arctic Ocean turns into a major source region for OCPs, and possible feedback affect the low latitude regions in the Northern Hemisphere;
- Oceanic water mass and riverine input contributed significantly to the Arctic OCPs;

1. Introduction

Legacy organochlorine pesticides (OCP)s are groups of anthropogenic chemicals that have been widely used and globally mass-produced. These compounds, which include HCHs and DDTs, have proved to be persistent and bioaccumulative in the environment, the potential for long-range atmospheric transport, and toxic to wildlife and humans (*Li et al.*, 1998; *Stemmler* and *Lammel*, 2009; *Willett et al.*, 1998). Because of their ecological and health risks, these pesticides started to be phased out globally apart from specific uses such as DDT for malaria vector control, and they have been added to the Persistent Organic Pollutants (POPs) list of the Stockholm Convention(*Cai et al.*, 2010; *Li et al.*, 2017; *Ma et al.*, 2018). Legacy OCPs have been detected globally in atmospheric, aquatic, and geological systems, and remote regions such as the Himalayas and polar regions(*Bailey et al.*, 2000; *Cai et al.*, 2012; *Gao et al.*, 2010; *Huang et al.*, 2013; *Li*, 1999; *Ren et al.*, 2019).

As is typical of OCPs, HCHs and DDTs can be transported to high-Arctic regions by long-range atmospheric transport (LRAT), ocean currents, and river runoff(*Cai et al.*, 2010; *Cai et al.*, 2012; *Huang et al.*, 2013; *Stemmler and Lammel*, 2009). These processes involve a sequence of temperature-dependent volatilization processes known as the "grass hopping effect" (*Wania and Mackay*, 1996). Atmospheric circulation is the most rapid transport pathway, and the "cold-trapping effect" in high-latitude regions drives the gaseous phase to partition with snow, ice, rain, seawater, soils, and vegetation, extending the retention time of OCPs(*Kang et al.*, 2012; *Wania*, 1997; *Wania and Mackay*, 1996). OCPs transported by the ocean currents, which have a higher carrying capacity and a bidirectional transport exchange, was much more than that by the air-sea exchange at the vast air-sea interface(*Bidleman et al.*, 2007; *Jaward et al.*, 2004; *Lohmann et al.*, 2012). For

example, ocean currents passing through the Bering Strait make a significant contribution to the input of OCPs to the Arctic Ocean, particularly for β-hexachlorocyclohexane (β-HCH)(*Li et al.*, 2002). River runoff carries land-based OCPs from soils, dry or wet absorption, and snow and ice melt-water into the large Arctic drainage basin which arguably is mostly the result of prior LRAT(*Cai et al.*, 2012; *Lambert et al.*, 2019; *Ma et al.*, 2018). OCPs from atmospheric, oceanic, and riverine sources thus converge in the Arctic Ocean(*Bidleman et al.*, 2015; *Cabrerizo et al.*, 2018; *Hung et al.*, 2016), with Arctic regions acting as reserves and secondary sources of OCPs(*Ma et al.*, 2016).

Global transport, distribution, redispersion, degradation, biological pump, and physical pump (subduction of deep waters) of OCPs are related to temperature, seawater salinity, and sea-ice extent(*Ma et al.*, 2004b; *Wania and Mackay*, 1996; *Wu et al.*, 2010). Furthermore, changes to the Arctic, a climate-sensitive region, may have a significant influence on the fate of OCPs by amplifying the effect of global climate change(*Dai et al.*, 2019; *Graversen and Wang*, 2009). OCPs resident in the ice or snow would be released into surface seawater or atmosphere once again. Moreover, the residence of OCPs in seawater below sea-ice, which get 2-5 times the fugacity of escape tendency than that of the equilibrium state, would also escape into the air much more rapidly(*Macdonald et al.*, 2005). Sea-ice melting releases HCHs and DDTs in snow and ice into surface seawater and the atmosphere, increasing air-sea exchange(*Bigot et al.*, 2017; *Wu et al.*, 2010). It is estimated that more than 2.6 Mt of DDTs and 8.4 Mt of HCHs have to get into the environment, with a significant fraction now being stored in the Antarctic and Arctic seawater, air, snow, and ice(*Li and Macdonald*, 2005; *Peterle*, 1969; *Voldner and Li*, 1995). Environmental changes in the Arctic Ocean are projected to enhance the subsequent release of OCPs with substantial effects on fragile Arctic ecosystems(*Ma and Cao*, 2010; *Ma et al.*, 2004a; *Ma et al.*, 2004b; *Ma et al.*, 2016). The transport mechanisms of legacy OCPs in the Arctic Ocean and their rate of regression and response to environmental change in the Arctic are not well understood(*Jantunen et*

al., 2015; *Lohmann et al.*, 2007; *Ma et al.*, 2011). In the Arctic Ocean surface seawater, some OCPs (e.g., HCHs) could be removed by the biological degradation, hydrolysis, and subduction of water masses to the sediments, in which biological pump plays a significant role to determine the removal rate(*Dachs et al.*, 2002; *Galban-Malagon et al.*, 2013; *Harner et al.*, 1999; *Zhang et al.*, 2012).

To investigate OCPs in the marine boundary of the Northern Hemisphere, surface seawater and atmospheric samples were collected during Arctic expeditions in 2016 and 2017. Seven legacy OCPs were analyzed: α-hexachlorocyclohexane (α-HCH), β-HCH, γ-hexachlorocyclohexane (γ-HCH), δ-hexachlorocyclohexane (δ-HCH), *p,p'*-dichlorodiphenyltrichloroethane(*p,p'*-DDT),*p,p'*-dichlorodiphenyldichloroethylene(*p,p'*-DDE), and *p,p'*-dichlorodiphenyldichloroethane (*p,p'*-DDD). The aims of the study were (1) to provide a large-scale distribution map of OCPs in the maritime boundary from East Asia to the Arctic Ocean; (2) to elucidate seasonal variations and sources of OCPs; and (3) to quantify the air-sea exchange flux of OCPs in the Arctic Ocean and provide a contour diffusion forecast map.

2. Data and Methods

2.1.Sample collections and Analytical Procedures

90 Surface seawater (stations A01–74, B01–16) and 16 atmospheric samples (stations C01–16) were collected from East Asia to the Arctic Ocean during voyages of the Chinese research vessel *Xue Long* (*Snow Dragon)* during the 7th and 8th Chinese National Arctic Research Expeditions of July 12 to September 23, 2016, and July 27 to October 7, 2017 (Support Information (SI): *TablesS1–S3 and Fig.S1-2*). Seawater and atmospheric samples were concentrated in a ship-borne laboratory using a high-volume solid-phase extraction method with the *in situ* internal ultrasonic (*Hi-volume SPE ISIU*) treatment (*Gao et al.*, 2019, *Cai, 2017a, Cai, 2017b, Cai, 2018, Zhang et al., 2020*) (*Text S1, Fig. S3*). Detailed descriptions of the sampling and concentration processes are given in the SI: *Text S2a-e* and *Fig. S4*. The laboratory analytical procedures for the OCP (*SI Text 2f*, selected-ion model: *Table S4*), field and laboratory blanks (*Text S2g*), contamination precautions (*SI Text*

2h), and laboratory contrast were present in the *SI*.

2.2.Model and Software Analysis Framework

Air masses were tracked for each atmospheric sample using HYSPLIT modeling (National Oceanic and Atmospheric Administration; NOAA), with 240-h back-trajectories at heights of 50, 500, and 1000 m. Retention time data (by the hour) originated from the back-trajectories, along with coordinate information, was input to the Meteo-InfoLab (Chinese Academy of Meteorological Sciences) software to determine source region impact factors (SRIFs). The diffusion and movement of selected OCPs in surface seawater in the eastern Arctic Ocean were estimated for the 2016 cruise using ArcGIS software (ESRI Co.). Kriging interpolation was applied to the analysis of ocean current movements(*Zheng et al.*, 2017) (*Text S3*). States of OCP phase equilibrium at the air-water interface were estimated using the fugacity computing method based on Whitman two-film theory(*Li et al.*, 2017; *Odabasi et al.*, 2008). Detailed descriptions of the air-sea exchange flux calculations are provided in the Supporting Information (*Text S4*).

3. Results

3.1.OCP Levels, Spatial Distribution Patterns, and Seasonal Variations in the Surface Seawater

The concentrations of HCHs and DDTs recorded in surface seawater along the 7th and 8th cruise tracks are shown in *Fig. 1a–c* and *Tables S6, S7*. During the 7th Arctic Expedition cruise (2016), 74 surface seawater samples were collected including 26 on the forward voyage from East Asia to the high Arctic Ocean (stations A01–26 with sampling dates of July 12 to August 7; *Fig. 1a*) and 48 on the return voyage (stations A27–74 with sampling dates of August 19 to September 23; *Fig. 1b*). Seven OCPs were below detection limits (BDL) at station A65. Total concentrations of the seven OCPs (Σ_7OCPs) during the outward voyage ranged from 0.12 ng L^{-1} (station A22; Canada Basin) to 12.39 ng L^{-1} (station A01; Tsushima Strait), with a mean of 2.93 ± 2.56 ng L^{-1}. Total concentrations of the four HCHs (Σ_4HCH) ranged from BDL to 9.32 ng L^{-1} (mean 1.28 ± 1.32 ng L^{-1}), similar to concentrations recorded in

2008, whereas the total concentrations of the three DDTs (Σ_3DDTs) were lower than those recorded in the Arctic Ocean in 2008(*Cai et al.*, 2010).

During the forward voyage, seawater concentrations of Σ_7OCPs decreased with increasing latitude from the Tsushima Strait to the Bering Sea, before decreasing sharply in the high Arctic Ocean after a slight increase in the Chukchi Sea. γ-HCH was the most abundant OCP with a mean concentration of 0.77 ± 0.57 ng L^{-1}(*Table S8 and Fig. S5a*), consistent with the fact that lindane (>90% γ-HCH) was still used in the early 2000s with Northern Hemisphere soil being a secondary source(*Breivik and Wania*, 2002; *Vizcaino and Pistocchi*, 2010). The levels of α-HCH generally increased with latitude in surface seawater, while the other six OCPs decreased with latitude increasing. The climbing levels of α-HCH is consistent with other analyses from the same region(*Cai et al.*, 2010; *Cai et al.*, 2012). Compared to previous studies, concentrations of α- HCH along the Bering Sea to the Arctic Ocean transect was much lower than that sampling in 1988, 1993, and 1999, but higher than that sampling in 2010 (*Table S9*). The result was in accord with the fate of the usage of α-HCH: start to be phased out at the end of the last century, but still be used in Asia regions(*Hargrave et al.*, 1997; *Hinckley et al.*, 1991; *Yao et al.*, 2002). α-HCH is more volatile and less water-soluble, so it less likely to be deposited in low-latitude regions and more likely to converge in the Arctic Ocean after LRAT and air-sea exchange. The concentration of *p,p'*-DDT in the Japan Sea (0.38 ± 0.19 ng L^{-1}) was much higher than that in the Northwest Pacific–Bering Sea (0.15 ± 0.02 ng L^{-1}) and the Chukchi Sea–Arctic Ocean (0.11 ± 0.08 ng L^{-1}) regions. During the forward voyage, concentrations of all DDTs in the was comparable to the previous studies in 2008 along the Bering Sea- Chukchi Sea(*Cai et al.*, 2010) (*Table S9*). However, p.p'-DDT in the Japan Sea was much higher than that in previous studies, which indicate there was a point source of p.p'-DDT near the Japan Sea.

(Place Figure 1 here.)

During the return voyage (2016) from the high Arctic Ocean to East Asia, the Σ_7OCP concentration ranged from BDL (station A65, Tsugaru Strait) to 3.12 ng L^{-1} (station A41, Canada Basin) with a mean of 0.87 ± 0.76 ng L^{-1}, which was one-third of that recorded on the outward voyage, indicating a significant seasonal variation. There were no obvious trends with the latitude of the Σ_7OCP during the return voyage. γ-HCH (0.27 ± 0.24 ng L^{-1}) was the most abundant contaminant, as was observed on the forward voyage (*Fig. S5b*). Seawater α-HCH concentrations decreased with decreasing latitude, in agreement with the trend recorded on the outward voyage. Spatial trends of the other six OCPs differed slightly from those recorded on the outward voyage, specifically those of β-, γ-, δ-HCH, and the three DDTs. The concentrations of individual OCP along the Arctic Ocean to Bering Sea transect did not vary significantly in contrast to the forward voyage. It presents a similar trend contrasting to the previous studies (*Table S9*). However, the seasonal spatial variations of OCPs concentrations in East Asia transect were significant. This might be attributed to the more agricultural activities in East Asia and mass pest control operations in the early autumn.

In order to verify the seasonal spatial variations of the OCP concentrations in surface seawater, repeated sampling work was conducted during the return voyage from September 12 to October 06 in 2017 (*Fig.1c, Table S2*). The highest Σ_7OCP concentration recorded was 3.71ng L^{-1} at station A06 (Chukchi Sea), with a mean of 1.03 ± 1.15 ng L^{-1}(*Table S7*). During the whole voyage, concentrations of HCHs (0.83 ± 0.97 ng L^{-1}) were still higher than DDTs (0.19 ± 0.19 ng L^{-1}), which were comparable with those of the 2016 return voyage. However, β-HCH (0.32 ± 0.41 ng L^{-1}) was the most abundant contaminant, with a higher concentration than that recorded in 2016 (0.16 ± 0.14 ng L^{-1}; *Fig. S5c, Table S8*). The Arctic Ocean–Chukchi Sea transect had the highest concentrations of Σ_7OCPs at over ten times those of the Bering Sea–Northwest Pacific transect, and four times those at low latitudes on the Japan Sea–East China Sea transect. Along the Chukchi Sea to the high Arctic Ocean, β-HCH and *p,p′*-DDD levels were about 2-3 times higher than

that recorded in 2016. The significantly climbing up concentrations may be due to ocean-current transport from the Bering Sea in the summer, rather than air-sea exchange and LRAT(*Li et al.*, 2002).

3.2. Levels and Spatial Distribution in the Marine Boundary Atmosphere

Atmospheric samples were taken during the 8th Arctic cruise (from July 27 to October 07, 2017), covering the central Arctic Ocean (Fig. 1d). All seven OCPs were above detection limits at all stations, with Σ_7OCP concentrations ranging from 0.1 to 1.21 ng m^{-3} (mean 0.35 ± 0.3 ng m^{-3}; Table S10). On the forward voyage (stations C01–09), Σ_7OCP concentrations ranged from 0.14 to 0.34 ng m^{-3} (mean 0.23 ± 0.09 ng m^{-3}, Fig. S5d), with an apparent decreasing trend from the Bering Sea to the West Norway Sea. The Arctic Ocean close to Alaska and the Russian Far East had higher levels of HCH and DDT contamination, with a distribution pattern similar to that reported by the international Arctic Monitoring and Assessment Program (AMAP) with concentrations of OCPs at Point Barrow and Valkarkat generally being higher than those at Alert and Zeppelin(*Hung et al.*, 2016). Σ_4HCHs (0.15 ± 0.03 ng m^{-3}) were the predominant contaminants, with β-HCH having higher concentrations across the Arctic Ocean than the other OCPs, possibly because of the introduction of oceanic water from the Pacific and Atlantic oceans, and the riverine input from the Russian rivers(*Li and Macdonald*, 2005; *Li et al.*, 2002).

During the return voyage in 2017 (stations C10–16), atmospheric Σ_7OCP concentrations ranged from 0.1 ng m^{-3} (station C10; Chukchi Sea) to 1.21 ng m^{-3} (station C16; the East China Sea close to Shanghai, China) with an overall mean of 0.50 ± 0.41 ng m^{-3}(Fig. S3e). The Japan Sea had the highest Σ_7OCP concentrations, at over ten times those recorded in the Chukchi Sea. Unlike the OCP composition recorded on the forward voyage, Σ_3DDTs (0.50 ± 0.40 ng m^{-3}) were predominant, and *p,p'*-DDT concentrations were significantly higher in low-latitude regions, indicating that agricultural activities in early autumn are a possible source.

3.3. Sources and degradation of OCPs in surface seawater

The α-HCH/γ-HCH ratio is commonly used to identify new sources of HCH

release to the environment and their extent to the degradation, with ratios < 1 indicating the primary source is the application of lindane, ratios>1 indicating the primary source is the application of technical HCHs (*Dickhut et al.,2005, Li et al., 2020*). Technical DDT comprises mainly *p,p'*-DDT (>85%), which degrades to DDD by reducing dechlorination under anaerobic conditions and metabolizes to DDE under aerobic conditions. A (DDD + DDE)/DDT ratio <1 indicates a new DDT source, whereas ratios >1 indicate that most of the legacy DDT has been degraded (*Mahmood et al.*, 2014).

During the 7th Arctic cruise (2016), the α-HCH/γ-HCH ratios were 0.08–1.69 (*Fig.2a*). Stations in the Chukchi Sea and Canada Basin (A17, A20, A21, A22, A26, A27, A30-32, A35-39, A42, and A43) displayed the ratios >1, which indicated the increasing input of the technical HCHs. Increases in these ratios with latitude were observed during both voyages and are attributed to increasing input from potential LRAT in high-Arctic regions, which is consistent with the observed increasing α-HCH and decreasing γ-HCH concentrations. The ratios were compared with those recorded on similar transects in 2008(*Cai et al.*, 2010). During the return voyage of the 8th Arctic cruise (2016), α-HCH/γ-HCH ratios were in the range 0.18–1.27, with a slightly increasing trend observed from East Asia to the Bering Sea transect (C13-16). B03 (Chukchi Sea) and B08 (southwest Bering Sea) got the ratios of α-HCH/γ-HCH over 1, suggesting a point contamination source for technical HCHs. The abrupt increase of the α-HCH/γ-HCH ratio in the Chukchi Sea possibly attributable to continental ice/snow melt-water. Along with East Asia to the Bering Sea low-latitude transect, ratios were below 1 during both cruises in 2016 and 2017, indicating that there must have been a persistent lindane source in low-latitude regions over recent years.

The (DDD + DDE)/DDT ratio follows a pattern different from that of the HCHs, with a range of 0.26–5.88 (*Fig.2a*, the red dot line means the ratio >1). Ratios were >1 in low-latitude regions of East Asia during the 2016 outward voyage, indicating substantial degradation of *p,p'*-DDT by increasing UV exposure and rising

temperatures in summer. Some samples, collected during surface-ice melting in the Arctic Ocean, had high ratios during both the forward and returned voyages, as *p,p'*-DDT stored beneath the surface sea-ice was re-exposed to air with accelerated degradation to *p,p'*-DDD and *p,p'*-DDE(*Geisz et al.*, 2008; *Hung et al.*, 2016; *Wu et al.*, 2010). The (DDD + DDE)/DDT ratios at most middle-latitude stations were <1, indicating new sources in the vicinity, which are possibly due to rising temperatures that cause DDTs in the soil to volatilize and also to be released into land runoff(*Luo et al.*, 2019; *Ren et al.*, 2019; *Vizcaino and Pistocchi*, 2010). The use of dicofol, with impurities that include *p,p'*-DDT, in China and Russia during the late spring and summer could also be a potential source(*Qiu et al.*, 2005; *Zheng et al.*, 2010). This region is also a busy shipping route, and thus *p,p'*-DDT in ship anti-corrosion treatments might also be a source(*Zheng et al.*, 2010). During the 2017 voyage, the trend in ratios with latitude was similar to that recorded in 2016, except for two stations in the Bering Sea close to Russia (stations B07 and B08) where low observed OCP concentrations might be attributable to lower levels of agricultural activities in the Russian Far East and the movement of coastal currents. By combining the ratio of HCHs and DDTs with the latitude, the correlation of α-HCH/γ-HCH ratios with latitude is significant. It suggests that technical HCHs are likely to accumulate as a primary source, and the transfer function of LRAT in cold regions becomes more durable with increasing latitude.

3.4. Atmospheric source analysis and back trajectories

Atmospheric OCPs have shorter half-lives, more complex transport pathways, and more sources than those in seawater, as their transport to the Arctic Ocean involves dry/wet deposition and air-sea exchange. The rainfall, snowfall, and air-sea exchange would retain the OCPs temporarily and then act as second sources driving the OCPs to continue with the LRAT(*Ma et al.*, 2016). Atmospheric α-HCH/γ-HCH ratios were in the range 0.33–3.33 (*Fig. 2b*) over the whole sampling period of the 8th Arctic cruise (2017). The trend of ratios got a slight difference from those in surface seawater in the Bering Sea in 2016. The primary source of HCHs, from East Asia to

the high Arctic Ocean, was the application of γ-HCH. The atmospheric α-HCH/γ-HCH ratios were lower than those observed in similar ocean transects in 2008 (1.3–4.8)(*Wu et al.*, 2010), 2003 (1.2–8.1)(*Ding et al.*, 2007), and 1993 (4.0–26)(*Li et al.*, 2006). This decrease in ratios over 20 years may be due to the phase-out of HCHs with continued use of lindane. Ratios in mid-latitude regions were higher than those at low latitudes, with γ-HCH being more likely to enter surface seawater by wet/dry deposition than is α-HCH.

Atmospheric (DDD + DDE)/DDT ratios were in the range 0.29–2.0 (*Fig.2b*), lower than values recorded in the previous studies(*Ding et al.*, 2009). Ratios <1 at stations C03, C05, C07, and C11 indicate a new source of atmospheric DDT in high-latitude regions. Air-mass back trajectories (*Fig.S6*) indicate potential sources of atmospheric *p,p'*-DDT along with Russian Arctic areas where large amounts of DDTs have been preserved since the last century(*Iwata et al.*, 1995) and could become secondary sources in the Northern Hemisphere summer(*Ma et al.*, 2016). (DDD + DDE)/DDT ratios at stations in the central Arctic Ocean (stations C4, C6, and C10) and North Europe (C8 and C9) were >1. It indicates that the legacy pp'-DDT has been degraded elsewhere or on transport to this sampling location.

(Place Figure 2 here.)

SRIFs have been widely applied to estimations of the environmental impacts of atmospheric pollutant source regions(*Bailey*, 2001; *Genualdi et al.*, 2009; *Primbs et al.*, 2007). Higher SRIF values indicate air masses with longer duration in the area before sampling and a higher probability of being the source region. SRIFs would demonstrate the global scale of source region partition in the Northern Hemisphere. Moreover, the global map was divided into several source regions (*Fig. S7*), which are defined as (A) Europe; (B) North Africa; (C) West Russia; (D) Middle East-West Asia; (E) East Russia and coastal regions; (F) East Asia; (G) North Pacific Ocean; (H) Canada and Alaska; (I) USA and middle Latin America; (J) Arctic; and (K) Southern

Hemisphere.

The relative contributions of the various source regions to atmospheric OCP concentrations in the Northern Hemisphere were as follows : J (56.33%) > E (11.36%) > H (10.07%) > G (9.64%) > F (7.74%) > A (2.4%) > C (1.39%) > D (0.66%) > I (0.29%) > B = K(0%)(Table S11). The Arctic region made the most significant contribution to the potential source of legacy OCPs contamination in the Northern Hemisphere. North Africa and the Southern Hemisphere had no impact on the marine boundary atmosphere in the survey area. Regions E and F made significant contributions because they retain large quantities of legacy OCPs. An overview of the back trajectories across the Arctic Ocean (stations C03–09; *Fig. 2c*) indicates that air-masses originated mainly from the Arctic Ocean, with the Arctic ocean itself turned into a significant potential source of legacy OCPs. In low-latitude regions of East Asia and the Japan Sea, China and Siberia were important source regions which contributed land-based OCPs to the marine atmosphere.

3.5. Air-sea Exchange in paired stations in the Chukchi Sea

Sea ice was at its minimum extent during the 2016 and 2017 summer sampling periods (*Fig. S8*). Air-sea exchange fluxes were calculated for each OCP for paired atmospheric and surface seawater samples taken in the East Arctic Ocean during 2017 (*Table S12*). Henry's constant (H') values were corrected according to previous studies(*Cetin et al.*, 2006; *Pascaud et al.*, 2016). The wind speed mainly influenced K_{ol}, and the uncertainly of K_{ol} was calculated by the maximum and minimum wind speed, which was assumed to be ±112%. Ranges of air-sea flux values (ng m^{-2} d^{-1}) were as follows: α-HCH, 0.25–0.38; β-HCH, 0.16–0.79; γ-HCH, 0.13–0.26; δ-HCH, 1.10–3.31; *p,p'*-DDE, 0.4–2.39; *p,p'*-DDD, 2.53; and *p,p'*-DDT 4.69–23.46. All flux values were positive, indicating net volatilization from surface seawater to the atmosphere.

The air-sea flux of *p,p'*-DDT flux was highest. As indicated above, the (DDD + DDE)/DDT ratio was generally >1. Atmospheric concentrations of *p,p'*-DDT were relatively high in the Chukchi Sea–Arctic Ocean regions with the enhanced

exchange of dissolved *p,p'*-DDT from surface seawater to the atmosphere and degradation of *p,p'*-DDT. At the paired stations B03–C11, the total flux of OCPs was much higher than that at the other paired stations, possibly because of the more considerable temperature difference between seawater and air in situ. The fluxes of α-HCH were much lower than those recorded earlier in the Chukchi Sea: 26 ng m^{-2} d^{-1} in 1990 (*Hinckley et al.*, 1991) and 7 ng m^{-2} d^{-1} in 2010(*Cai et al.*, 2012). Fluxes of γ-HCH were negative in the Southern Ocean at about the same latitude as in 2014(*Bigot et al.*, 2016).

3.6 Surface Contour diffusion along the Chukchi Sea to Canada Basin

During the 2016 Arctic cruise, high-density sampling was completed in the Chukchi Sea- Canada Basin (stations A14–49) for comparison with models of OCP diffusion in surface seawater. The ArcGIS 10.5 (ESRI Co.) model was applied along with Kriging interpolation to produce a contour diffusion map for forecasting OCP distributions in the East Arctic Ocean.

The contour diffusion map for ΣHCHs (*Fig.2d*) indicated that levels of HCHs (0.10–0.80 ng L^{-1}) in the west of the Canada Basin were low, and that (2.20–2.90 ng L^{-1}) from the Alaska Coast to the central Arctic Ocean were high. There were three high-concentration areas in the Canada Basin. In the contour diffusion map for individual HCHs (*Fig. S9*), α-HCH displays a clear east-west difference, implying that the eastern Canada Basin may undergo severe contamination in the future, possibly from coastal runoff from Alaska or the Canadian Arctic Islands. Similar diffusion trends are evident for γ-HCH, which has sources near the Alaska coast.

The DDT contour diffusion map also displays zonal distribution patterns (*Fig. 2e*), with low concentrations (0.01–0.13 ng L^{-1}) in the west of the Canada Basin and the highest concentrations (0.27–0.31 ng L^{-1}) from the Bering Strait to the central Arctic Ocean. Among the diffusion maps of individual DDTs (Fig. S9), *p,p'*-DDT, *p,p'*-DDE, and *p,p'*-DDD patterns are consistent with the forecast ΣDDT distribution; and the *p,p'*-DDT and *p,p'*-DDD maps follow the delivery function of the Bering Sea and that of the land-based source of *p,p'*-DDE in Alaska. ΣDDTs and individual DDT

distribution maps were not consistent with the movement of surface ocean currents in the Arctic Ocean. The temperature distribution map (*Fig.S9*) indicates that water masses originating in the Bering Sea raise the temperature of the Arctic Ocean, providing a significant source of HCHs and DDTs in surface seawater. Correlations analysis indicates that most of the individual OCPs don't have strong positive correlations with salinity and the temperature of surface seawater. However, it is to be noticed that the concentration of β-HCH demonstrated a strong negative correlation to the salinity of the surface seawater, which indicated that the high concentration of β-HCH originated from the snow melting process and river discharge from Alaska, amplifying the concentrations.

4. Conclusion

This paper was the first updated field investigation along East Asia to the Arctic Ocean transect for the OCPs in the last decades. Levels of the total OCPs in both surface seawater and atmosphere indicated that reducing DDT contamination and comparative HCH contamination in contrast to the previous studies. The potential point source and agriculture activities in the early autumn made a significant contribution to the high levels of DDTs in East Asia. Along the sampling transect, the significant and rapid seasonal variation of the legacy OCPs in the surface seawater was first reported. The legacy OCPs concentrations in the Arctic Ocean gradually decreased with distance from water masses originating in the Bering Sea and the landmass of Alaska. Based on the atmospheric SRIFs value, air mass back trajectories, and the air-sea exchange, Japan, China, and Siberia were important source regions which contributed land-based OCPs to the marine atmosphere in the low latitude regions, and the Arctic Ocean turned into a significant potential source which could possible feedback affect the low latitude regions in the Northern Hemisphere. This paper would give an insight into the large-scale fraction of OCPs with climate change. However, more continuous field investigations are needed for a better understanding of the global fate of OCPs.

Acknowledgment

We wish to express our sincere gratitude to the crews of the 7th and 8th Chinese National Arctic Research Expeditions onboard R/V ***Xuelong*** for their great support during the *in situ* sampling collection. We would like to thank Dr. Xiangzhou Meng and Dr. Ningzheng Zhu (Jiaxing-Tongji Environmental Research Institute) for the data analysis assistance and discussions. This work was funded by the National Natural Science Foundation of China (Nos. 41776202, 91851201). All the sampling information, sample treatment, and analyzing results are accessible in the supporting information attached to this article. The data archiving is underway and all the data is open access in the Arctic Data Center (National Science Foundation Polar Programs, USA) https://arcticdata.io/.

References

Bailey, R., L. A. Barrie, C. J. Halsall, P. Fellin, and D. C. G. Muir (2000), Atmospheric organochlorine pesticides in the western Canadian Arctic: Evidence of transpacific transport, *J Geophys Res-Atmos*, 105(D9), 11805-11811, https://doi.org/10.1029/1999jd901180.

Bailey, R. E. (2001), Global hexachlorobenzene emissions, *Chemosphere*, 43(2), 167-182, https://doi.org/10.1016/S0045-6535(00)00186-7.

Bidleman, T. F., H. Kylin, L. M. Jantunen, P. A. Helm, and R. W. MacDonald (2007), Hexachlorocyclohexanes in the Canadian Archipelago. 1. Spatial distribution and pathways of alpha-, beta- and gamma-HCHs in surface water, *Environmental Science & Technology*, 41(8), 2688-2695, https://doi.org/10.1021/es062375b.

Bidleman, T. F., L. M. Jantunen, H. Hung, J. Ma, G. A. Stern, B. Rosenberg, and J. Racine (2015), Annual cycles of organochlorine pesticide enantiomers in Arctic air suggest changing sources and pathways, *Atmospheric Chemistry and Physics*, 15(3), 1411-1420, https://doi.org/10.5194/acp-15-1411-2015.

Bigot, M., D. C. G. Muir, D. W. Hawker, R. Cropp, J. Dachs, C. F. Teixeira, and S. B. Nash (2016), Air-Seawater Exchange of Organochlorine Pesticides in the Southern Ocean between Australia and Antarctica, *Environmental Science & Technology*, 50(15), 8001-8009, https://doi.org/10.1021/acs.est.6b01970.

Bigot, M., D. W. Hawker, R. Cropp, D. C. G. Muir, B. Jensen, R. Bossi, and S. M. B. Nash (2017), Spring Melt and the Redistribution of Organochlorine Pesticides in the Sea-Ice Environment: A Comparative Study between Arctic and Antarctic Regions, *Environmental Science & Technology*, 51(16), 8944-8952, https://doi.org/10.1021/acs.est.7b02481.

Breivik, K., and F. Wania (2002), Evaluating a model of the historical behavior of two hexachlorocyclohexanes in the Baltic sea environment, *Environmental Science & Technology*, 36(5), 1014-1023, https://doi.org/10.1021/es001971h.

Brubaker, W. W., and R. A. Hites (1998), OH reaction kinetics of gas-phase alpha- and gamma-hexachlorocyclohexane and hexachlorobenzene, *Environmental Science & Technology*, 32(6), 766-769, https://doi.org/10.1021/es970650b.

Cabrerizo, A., D. C. G. Muir, A. O. De Silva, X. W. Wang, S. F. Lamoureux, and M. J. Lafreniere (2018), Legacy and Emerging Persistent Organic Pollutants (POPs) in Terrestrial Compartments in the High Arctic: Sorption and Secondary Sources, *Environmental Science & Technology*, 52(24), 14187-14197, https://doi.org/10.1021/acs.est.8b05011.

Cai, M. G., C. R. Qiu, Y. Shen, M. H. Cai, S. Y. Huang, B. H. Qian, J. H. Sun, and X. Y. Liu (2010), Concentration and distribution of 17 organochlorine pesticides (OCPs) in seawater from the Japan Sea northward to the Arctic Ocean, *Science China-Chemistry*, 53(5), 1033-1047, https://doi.org/10.1007/s11426-010-0182-0.

Cai, M. H., Y. X. Ma, Z. Y. Xie, G. C. Zhong, A. Moller, H. Z. Yang, R. Sturm, J. F. He, R. Ebinghaus, and X. Z. Meng (2012), Distribution and air-sea exchange of organochlorine pesticides in the North Pacific and the Arctic, *J Geophys Res-Atmos*, 117, https://doi.org/ArtnD0631110.1029/2011jd016910.

Cai, M. H. (2017a). Apparatus for water sampling based on high-volume solid-phase extraction sampling column, China Patent, 201720407400.3(P). http://www.soopat.com/Patent/201720407400

Cai, M. H. (2017b). Apparatus for atmospheric sampling based on high-volume solid-phase extraction sampling column, China Patent. 201720407396.0(P), http://www.soopat.com/Patent/201720407396

Cai, M. H. (2018). Apparatuses for high-volume solid-phase extraction sampling column and in situ internal ultrasonic elution, China Patent, 201720406918.5(P). http://www.soopat.com/Patent/201720406918

Cetin, B., S. Ozer, A. Sofuoglu, and M. Odabasi (2006), Determination of Henry's law constants of organochlorine pesticides in deionized and saline water as a function of temperature, *Atmospheric Environment*, 40(24), 4538-4546, https://doi.org/10.1016/j.atmosenv.2006.04.009.

Dachs, J., R. Lohmann, W. A. Ockenden, L. Mejanelle, S. J. Eisenreich, and K. C. Jones (2002), Oceanic biogeochemical controls on global dynamics of persistent organic pollutants, Environmental Science & Technology, 36(20), 4229-4237, https://doi.org/10.1021/es025724k.

Dai, A. G., D. H. Luo, M. R. Song, and J. P. Liu (2019), Arctic amplification is caused by sea-ice loss under increasing CO2, *Nature Communications*, 10, https://doi.org/ARTN121 10.1038/s41467-018-07954-9.

Ding, X., X. M. Wang, Q. Y. Wang, Z. Q. Xie, C. H. Xiang, B. X. Mai, and L. G. Sun (2009), Atmospheric DDTs over the North Pacific Ocean and the adjacent Arctic region: Spatial distribution, congener patterns and source implication, *Atmospheric Environment*, 43(28), 4319-4326, https://doi.org/10.1016/j.atmosenv.2009.06.003.

Ding, X., X. M. Wang, Z. Q. Xie, C. H. Xiang, B. X. Mai, L. G. Sun, M. Zheng, G. Y. Sheng, and J. M. Fu (2007), Atmospheric hexachlorocyclohexanes in the North Pacific Ocean and the adjacent Arctic region: Spatial patterns, chiral signatures, and sea-air exchanges, *Environmental Science & Technology*, 41(15), 5204-5209, https://doi.org/10.1021/es070237w.

Galban-Malagon, C. J., N. Berrojalbiz, R. Gioia, and J. Dachs (2013), The "Degradative" and "Biological" Pumps Controls on the Atmospheric Deposition and Sequestration of Hexachlorocyclohexanes and Hexachlorobenzene in the North Atlantic and Arctic Oceans, *Environmental Science & Technology*, 47(13), 7195-7203, https://doi.org/10.1021/es4011256.

Gao, H., J. M. Ma, Z. H. Cao, A. Dove, and L. S. Zhang (2010), Trend and climate signals in seasonal air concentration of organochlorine pesticides over the Great Lakes, *J Geophys Res-Atmos*, 115, https://doi.org/Artn D1530710.1029/2009jd013627.

Gao, Y., H. Y. Zheng, Y. Y. Xia, M. Chen, X. Z. Meng, and M. H. Cai (2019), Spatial Distributions and Seasonal Changes of Current-Use Pesticides from the North Pacific to the Arctic Oceans, *J Geophys Res-Atmos*, 124(16), 9716-9729, https://doi.org/10.1029/2018jd030186.

Geisz, H. N., R. M. Dickhut, M. A. Cochran, W. R. Fraser, and H. W. Ducklow (2008), Melting glaciers: A probable source of DDT to the Antarctic marine ecosystem, *Environmental Science & Technology*, 42(11), 3958-3962, https://doi.org/10.1021/es702919n.

Genualdi, S. A., R. K. Killin, J. Woods, G. Wilson, D. Schmedding, and S. L. M. Simonich (2009), Trans-Pacific and Regional Atmospheric Transport of Polycyclic Aromatic Hydrocarbons and Pesticides in Biomass Burning Emissions to Western North America, *Environmental Science & Technology*, 43(4), 1061-1066, https://doi.org/10.1021/es802163c.

Graversen, R. G., and M. H. Wang (2009), Polar amplification in a coupled climate model with locked albedo, *Clim Dynam*, 33(5), 629-643, https://doi.org/10.1007/s00382-009-0535-6.

Hargrave, B. T., L. A. Barrie, T. F. Bidleman, and H. E. Welch (1997), Seasonality in exchange of organochlorines between Arctic air and seawater, *Environmental Science & Technology*, 31(11), 3258-3266, https://doi.org/10.1021/es970266e.

Harner, T., H. Kylin, T. F. Bidleman, and W. M. J. Strachan (1999), Removal of alpha- and gamma-hexachlorocyclohexane and enantiomers of alpha-hexachlorocyclohexane in the eastern Arctic Ocean, *Environmental Science & Technology*, 33(8), 1157-1164, https://doi.org/10.1021/es980898g.

Hinckley, D. A., T. F. Bidleman, and C. P. Rice (1991), Atmospheric Organochlorine Pollutants and Air-Sea Exchange of Hexachlorocyclohexane in the Bering and Chukchi Seas, *J Geophys Res-Oceans*, 96(C4), 7201-7213, https://doi.org/10.1029/90jc02642.

Huang, Y. M., Y. Xu, J. Li, W. H. Xu, G. Zhang, Z. N. Cheng, J. W. Liu, Y. Wang, and C. G. Tian (2013), Organochlorine Pesticides in the Atmosphere and Surface Water from the Equatorial Indian Ocean: Enantiomeric Signatures, Sources, and Fate, *Environmental Science & Technology*, 47(23), 13395-13403, https://doi.org/10.1021/es403138p.

Hung, H., et al. (2016), Temporal trends of Persistent Organic Pollutants (POPs) in arctic air: 20 years of monitoring under the Arctic Monitoring and Assessment Programme (AMAP), *Environmental Pollution*, 217, 52-61, https://doi.org/10.1016/j.envpol.2016.01.079.

Iwata, H., S. Tanabe, K. Ueda, and R. Tatsukawa (1995), Persistent Organochlorine Residues in Air, Water, Sediments, and Soils from the Lake Baikal Region, Russia, *Environmental Science & Technology*, 29(3), 792-801, https://doi.org/10.1021/es00003a030.

Jantunen, L. M., F. Wong, A. Gawor, H. Kylin, P. A. Helm, G. A. Stern, W. M. J. Strachan, D. A. Burniston, and T. F. Bidleman (2015), 20 Years of Air-Water Gas Exchange Observations for Pesticides in the Western Arctic Ocean, *Environmental Science & Technology*, 49(23), 13844-13852, https://doi.org/10.1021/acs.est.5b01303.

Jaward, F. M., J. L. Barber, K. Booij, J. Dachs, R. Lohmann, and K. C. Jones (2004), Evidence for dynamic air-water coupling and cycling of persistent organic pollutants over the open Atlantic Ocean, *Environmental Science & Technology*, 38(9), 2617-2625, https://doi.org/10.1021/es049881q.

Kang, J. H., M. H. Son, S. D. Hur, S. Hong, H. Motoyama, K. Fukui, and Y. S. Chang (2012), Deposition of organochlorine pesticides into the surface snow of East Antarctica, *Science of the Total Environment*, 433, 290-295, https://doi.org/10.1016/j.scitotenv.2012.06.037.

Lambert, E., A. Nummelin, P. Pemberton, and M. Ilicak (2019), Tracing the Imprint of River Runoff Variability on Arctic Water Mass Transformation, *J Geophys Res-Oceans*, 124(1), 302-319, https://doi.org/10.1029/2017jc013704.

Li, Y. F. (1999), Global gridded technical hexachlorocyclohexane usage inventories using a global cropland as a surrogate, *J Geophys Res-Atmos*, 104(D19), 23785-23797, https://doi.org/10.1029/1999jd900448.

Li, Y. F., and R. W. Macdonald (2005), Sources and pathways of selected organochlorine pesticides to the Arctic and the effect of pathway divergence on HCH trends in biota: a review, *Science of the Total Environment*, 342(1-3), 87-106, https://doi.org/10.1016/j.scitotenv.2004.12.027.

Li, Y. F., M. T. Scholtz, and B. J. van Heyst (2000), Global gridded emission inventories of alpha-hexachlorocyclohexane, *J Geophys Res-Atmos*, 105(D5), 6621-6632, https://doi.org/10.1029/1999jd901081.

Li, Y. F., T. F. Bidleman, L. A. Barrie, and L. L. McConnell (1998), Global hexachlorocyclohexane use trends and their impact on the arctic atmospheric environment, *Geophysical Research Letters*, 25(1), 39-41, https://doi.org/10.1029/97gl03441.

Li, Y. F., R. W. Macdonald, L. M. M. Jantunen, T. Harner, T. F. Bidleman, and W. M. J. Strachan (2002), The transport of beta-hexachlorocyclohexane to the western Arctic Ocean: a contrast to alpha-HCH, *Science of the Total Environment*, 291(1-3), 229-246, https://doi.org/10.1016/S0048-9697(01)01104-4.

Li, Y. F., A. V. Zhulidov, R. D. Robarts, L. G. Korotova, D. A. Zhulidov, T. Y. Yurtovaya, and L. P. Ge (2006), Dichlorodiphenyltrichloroethane usage in the Former Soviet Union, *Science of the Total Environment*, 357(1-3), 138-145, https://doi.org/10.1016/j.scitotenv.2005.06.009.

Li, Z. X., T. Lin, Y. Y. Li, Y. Q. Jiang, and Z. G. Guo (2017), Atmospheric deposition and air-sea gas exchange fluxes of DDT and HCH in the Yangtze River Estuary, East China Sea, *J Geophys Res-Atmos*, 122(14), 7664-7677, https://doi.org/10.1002/2016jd026330

Li Y. L., Lohmann R., Zou X. Q., Wang C. L., Zhang, L.,(2020), Air-water exchange and distribution pattern of organochlorine pesticides in the atmosphere and surface water of the open Pacific ocean, *Environmental Pollution, 265*, 114956, https://doi.org/10.1016/j.envpol.2020.114956

Lohmann, R., K. Breivik, J. Dachs, and D. Muir (2007), Global fate of POPs: Current and future research directions, *Environmental Pollution*, 150(1), 150-165, https://doi.org/10.1016/j.envpol.2007.06.051.

Lohmann, R., J. Klanova, P. Kukucka, S. Yonis, and K. Bollinger (2012), PCBs and OCPs on a East-to-West Transect: The Importance of Major Currents and Net Volatilization for PCBs in the Atlantic Ocean, *Environmental Science & Technology*, 46(19), 10471-10479, https://doi.org/10.1021/es203459e.

Luo, Y. D., R. Q. Yang, Y. M. Li, P. Wang, Y. Zhu, G. L. Yuan, Q. H. Zhang, and G. B. Jiang (2019), Accumulation and fate processes of organochlorine pesticides (OCPs) in soil profiles in Mt. Shergyla, Tibetan Plateau: A comparison on different forest types, *Chemosphere*, 231, 571-578, https://doi.org/10.1016/j.chemosphere.2019.05.181.

Ma, J. M., and Z. H. Cao (2010), Quantifying the Perturbations of Persistent Organic Pollutants Induced by Climate Change, *Environmental Science & Technology*, 44(22), 8567-8573, https://doi.org/10.1021/es101771g.

Ma, J. M., Z. H. Cao, and H. Hung (2004a), North Atlantic Oscillation signatures in the atmospheric concentrations of persistent organic pollutants: An analysis using Integrated Atmospheric Deposition Network-Great Lakes monitoring data, *J Geophys Res-Atmos*, 109(D12), https://doi.org/Artn D1230510.1029/2003jd004435.

Ma, J. M., H. Hung, and P. Blanchard (2004b), How do climate fluctuations affect persistent organic pollutant distribution in North America? Evidence from a decade of air monitoring, *Environmental Science & Technology*, 38(9), 2538-2543, https://doi.org/10.1021/es0349610.

Ma, J. M., H. Hung, and R. W. Macdonald (2016), The influence of global climate change on the environmental fate of persistent organic pollutants: A review with emphasis on the Northern Hemisphere and the Arctic as a receptor, *Global Planet Change*, 146, 89-108, https://doi.org/10.1016/j.gloplacha.2016.09.011.

Ma, J. M., H. L. Hung, C. Tian, and R. Kallenborn (2011), Revolatilization of persistent organic pollutants in the Arctic induced by climate change, *Nature Climate Change*, 1(5), 255-260,

https://doi.org/10.1038/Nclimate1167.

Ma, Y. X., et al. (2018), Concentrations and Water Mass Transport of Legacy POPs in the Arctic Ocean, *Geophysical Research Letters*, 45(23), 12972-12981, https://doi.org/10.1029/2018gl078759.

Macdonald, R. W., T. Harner, and J. Fyfe (2005), Recent climate change in the Arctic and its impact on contaminant pathways and interpretation of temporal trend data, *Science of the Total Environment*, 342(1-3), 5-86, https://doi.org/10.1016/j.scitotenv.2004.12.059.

Mahmood, A., R. N. Malik, J. Li, and G. Zhang (2014), Levels, distribution pattern and ecological risk assessment of organochlorines pesticides (OCPs) in water and sediments from two tributaries of the Chenab River, Pakistan, *Ecotoxicology*, 23(9), 1713-1721, https://doi.org/10.1007/s10646-014-1332-5.

Odabasi, M., B. Cetin, E. Demircioglu, and A. Sofuoglu (2008), Air-water exchange of polychlorinated biphenyls (PCBs) and organochlorine pesticides (OCPs) at a coastal site in Izmir Bay, Turkey, *Mar Chem*, 109(1-2), 115-129, https://doi.org/ 10.1016/j.marchem.2008.01.001.

Pascaud, A., S. Sauvage, P. Coddeville, M. Nicolas, L. Croise, A. Mezdour, and A. Probst (2016), Contrasted spatial and long-term trends in precipitation chemistry and deposition fluxes at rural stations in France, *Atmospheric Environment*, 146, 28-43, https://doi.org/10.1016/j.atmosenv.2016.05.019.

Peterle, T. J. (1969), DDT in Antarctic snow, *Nature*, 224(5219), 620. https://doi.org/10.1038/224620a0

Primbs, T., S. Simonich, D. Schmedding, G. Wilson, D. Jaffe, A. Takami, S. Kato, S. Hatakeyama, and Y. Kajii (2007), Atmospheric outflow of anthropogenic semivolatile organic compounds from East Asia in spring 2004, *Environmental Science & Technology*, 41(10), 3551-3558, https://doi.org/10.1021/es062256w.

Qiu, X. H., T. Zhu, B. Yao, J. X. Hu, and S. W. Hu (2005), contribution of dicofol to the current DDT pollution in China, *Environmental Science & Technology*, 39(12), 4385-4390, https://doi.org/10.1021/es050342a.

Ren, J., X. P. Wang, P. Gong, and C. F. Wang (2019), Characterization of Tibetan Soil As a Source or Sink of Atmospheric Persistent Organic Pollutants: Seasonal Shift and Impact of Global Warming, *Environmental Science & Technology*, 53(7), 3589-3598, https://doi.org/10.1021/acs.est.9b00698.

Stemmler, I., and G. Lammel (2009), Cycling of DDT in the global environment 1950-2002: World ocean returns the pollutant, *Geophysical Research Letters*, 36, https://doi.org/Artn L2460210.1029/2009gl041340.

Vizcaino, P., and A. Pistocchi (2010), A GIS model-based assessment of the environmental distribution of gamma-hexachlorocyclohexane in European soils and waters, *Environmental Pollution*, 158(10), 3017-3027, https://doi.org/10.1016/j.envpol.2010.07.018.

Voldner, E. C., and Y. F. Li (1995), Global Usage of Selected Persistent Organochlorines, *Science of the Total Environment*, 160-61, 201-210, https://doi.org/10.1016/0048-9697(95)04357-7.

Walker, K., D. A. Vallero, and R. G. Lewis (1999), Factors influencing the distribution of lindane and other hexachlorocyclohexanes in the environment, *Environmental Science & Technology*, 33(24), 4373-4378, https://doi.org/10.1021/es990647n.

Wania, F. (1997), Modelling the fate of non-polar organic chemicals in an ageing snow pack,

Chemosphere, 35(10), 2345-2363, https://doi.org/10.1016/S0045-6535(97)00312-3.

Wania, F., and D. Mackay (1996), Tracking the distribution of persistent organic pollutants, *Environmental Science & Technology*, 30(9), A390-A396, https://doi.org/10.1021/es962399q.

Willett, K. L., Ulrich, E. M, and R. A. Hites (1998), Differential Toxicity and Environmental Fates of Hexachlorocyclohexane Isomers, *Environmental Science & Technology*, 32(15), 2197-2207.

Wu, X. G., J. C. W. Lam, C. H. Xia, H. Kang, L. G. Sun, Z. Q. Xie, and P. K. S. Lam (2010), Atmospheric HCH Concentrations over the Marine Boundary Layer from Shanghai, China to the Arctic Ocean: Role of Human Activity and Climate Change, *Environmental Science & Technology*, 44(22), 8422-8428, https://doi.org/10.1021/es102127h.

Yao, Z. W., G. B. Jiang, and H. Z. Xu (2002), distribution of organochlorine pesticides in seawater of the Bering and Chukchi Sea, *Environmental Pollution*, 116(1), 49-56.

Zhang, L., T. Bidleman, M. J. Perry, and R. Lohmann (2012), Fate of Chiral and Achiral Organochlorine Pesticides in the North Atlantic Bloom Experiment, Environmental Science & Technology, 46(15), 8106-8114, https://doi.org/10.1021/es3009248

Zhang S.W., Zhu N.Z., Zheng H.Y, Gao Y., Du H.N., Cai M.H., and Meng X.Z (2020), Occurrence of seventy-nine SVOCs in tapwater of China based on high throughput organic analysis testing combined with high volume solid phase extraction, *Chemosphere*, 256, 127-136, https://doi.org/10.1016/j.chemosphere.2020.127136

Zheng, H. Y., F. Wang, Z. Zhao, Y. X. Ma, H. Z. Yang, Z. B. Lu, M. G. Cai, and M. H. Cai (2017), Distribution profiles of per- and poly fluoroalkyl substances (PFASs) and their re-regulation by ocean currents in the East and South China Sea, *Marine Pollution Bulletin*, 125(1-2), 481-486, https://doi.org/10.1016/j.marpolbul.2017.08.009.

Zheng, X. Y., D. Z. Chen, X. D. Liu, Q. F. Zhou, Y. Liu, W. Yang, and G. B. Jiang (2010), Spatial and seasonal variations of organochlorine compounds in air on an urban-rural transect across Tianjin, China, *Chemosphere*, 78(2), 92-98, https://doi.org/10.1016/j.chemosphere.2009.10.017.

Figure Captions:

Figure 1 The spatial distribution of 7 selected OCPs from East Asia to the Arctic Ocean: (a) surface seawater samples during the forward voyage of the 7th Chinese National Arctic Expedition Cruise in 2016; (b) surface seawater samples during the backward voyage of the 7th Chinese National Arctic Expedition Cruise in 2016; (c) surface seawater samples during the backward voyage of the 8th Chinese National Arctic Expedition Cruise in 2017; (d) atmosphere samples during the whole cruise of the 8th Chinese National Arctic Expedition Cruise in 2017 (C01-09, forward voyage across the Arctic Ocean; C10-16, return voyage from the Arctic Ocean to East Asia).

Figure 2 (a)The α-HCH/γ-HCH and (DDD+DDE)/DDT ratios in the surface seawater samples from East Asia to the Arctic Ocean during both cruises in 2016 and 2017; (b) The α-HCH/γ-HCH and (DDD+DDE)/DDT ratios in the atmosphere samples from East Asia to the Arctic Ocean during the return voyage (C01-16) in 2017; (c) The summary of air-mass back trajectories of the samples across the Arctic Ocean during the Cruise in 2017; (d) The contour diffusion map of total HCHs in the surface seawater of the East Arctic Ocean (A14-49) in 2016; (d) The contour diffusion map of total DDTs in the surface seawater of the East Arctic Ocean (A14-49) in 2016.

Figure 1a-b

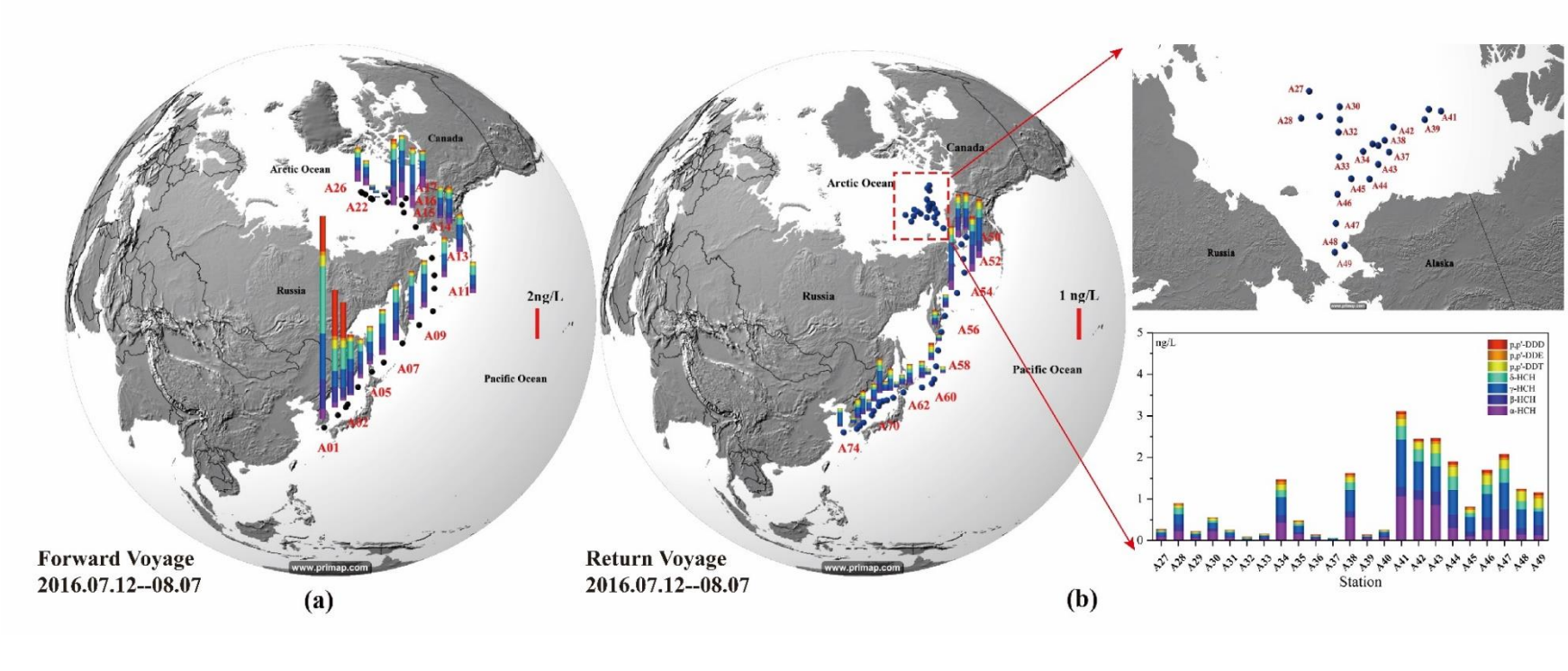
Forward Voyage
2016.07.12--08.07
(a)
Arctic Ocean
Canada
Russia
Pacific Ocean
2ng/L
A26
A22
A13
A11
A09
A07
A05
A02
A01
Return Voyage
2016.07.12--08.07
(b)
Arctic Ocean
Canada
Russia
Pacific Ocean
1 ng/L
A52
A54
A56
A58
A60
A62
A70
A74
Russia
Alaska
ng/L
p,p'-DDD
p,p'-DDE
p,p'-DDT
δ-HCH
γ-HCH
β-HCH
α-HCH
Station

Figure 1c-d

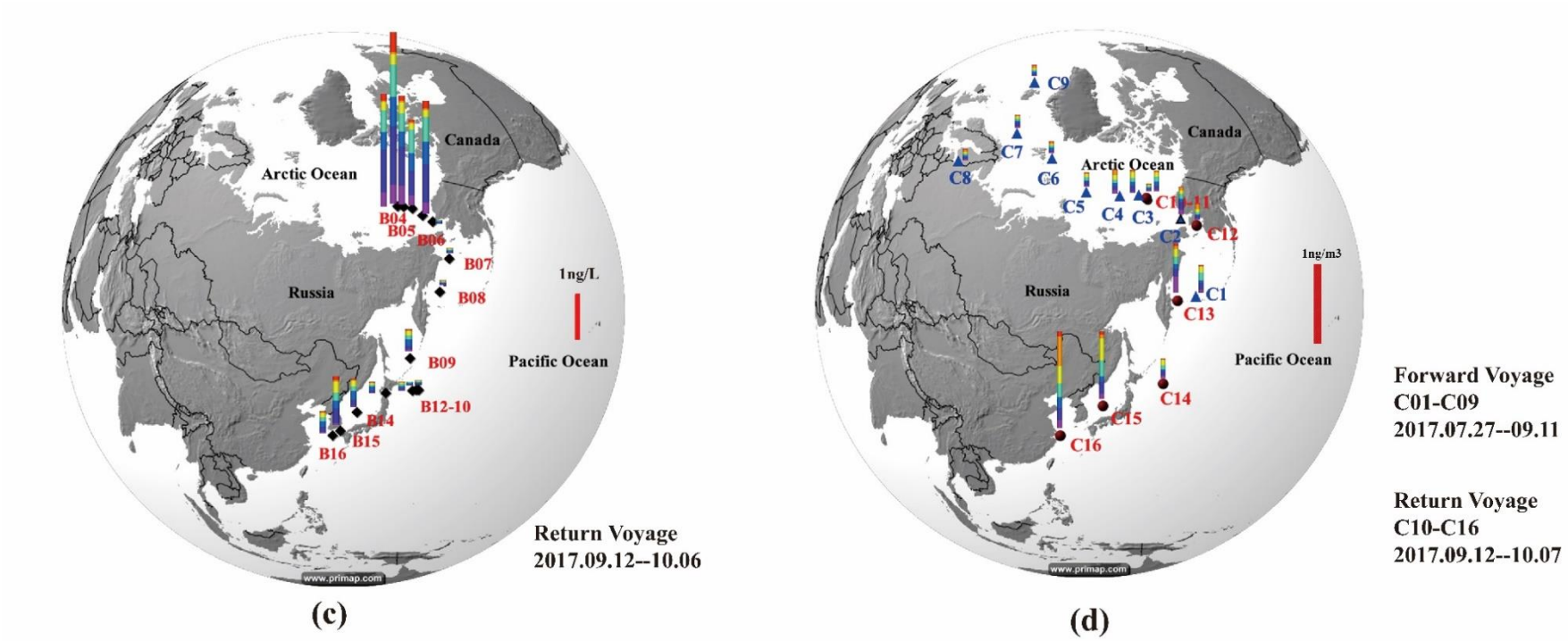
Canada
Arctic Ocean
Russia
Pacific Ocean
B04
B05
B06
B07
B08
B09
B12-10
B14
B15
B16
1ng/L
Return Voyage
2017.09.12--10.06
www.primap.com
(c)
C9
C7
C8
C6
C5
C4
C3
C2
C1
C12
C13
C14
C15
C16
1ng/m3
Forward Voyage
C01-C09
2017.07.27--09.11
Return Voyage
C10-C16
2017.09.12--10.07
(d)

Figure 2

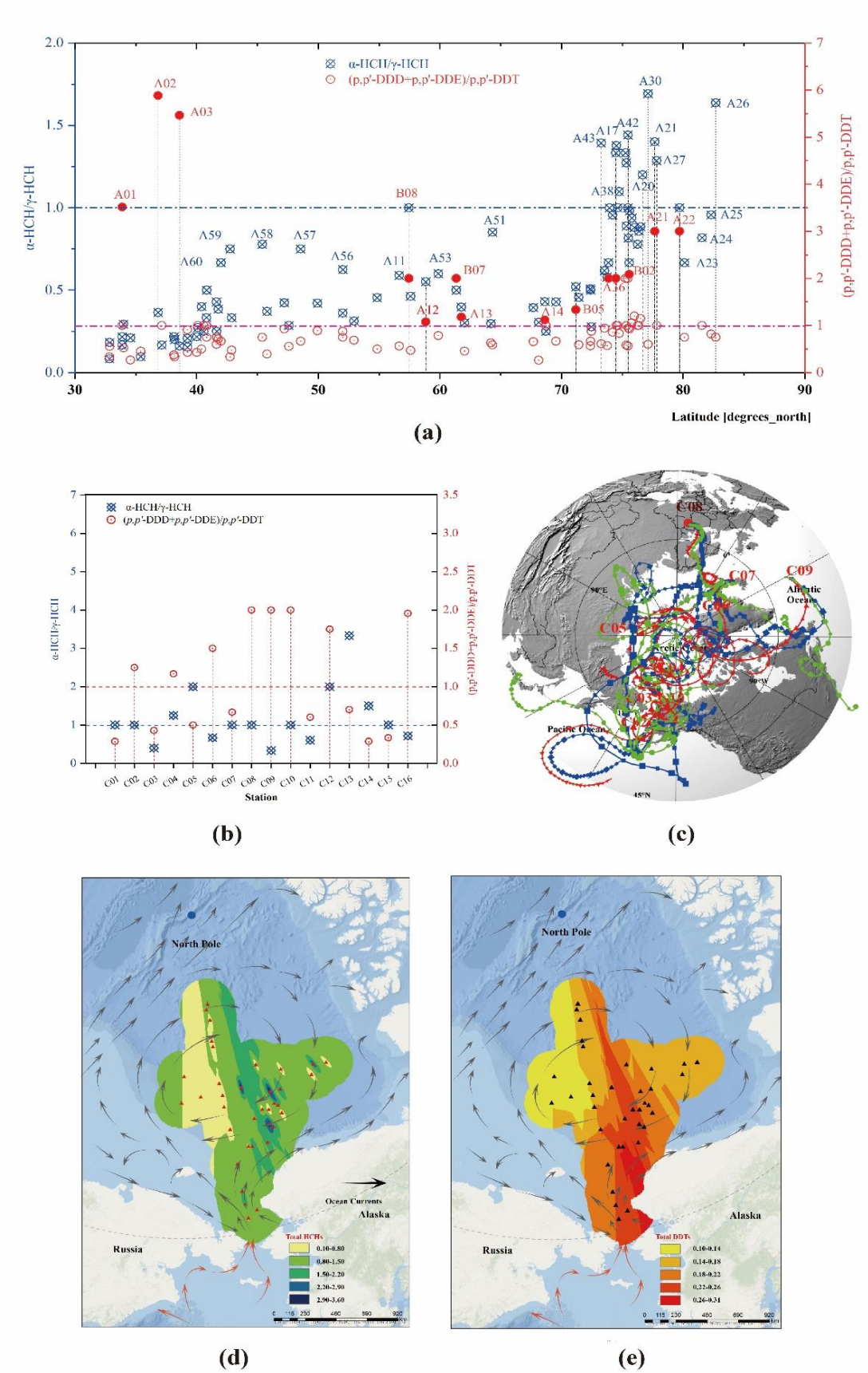
α-HCH/γ-HCH
(p,p'-DDD+p,p'-DDE)/p,p'-DDT
Latitude [degrees_north]
(a)
Station
(b)
Pacific Ocean
Atlantic Ocean
(c)
North Pole
Ocean Currents
Alaska
Russia
Total HCHs
Total DDTs
(d)
(e)

Support Information:Figures

Seasonal Variation of Legacy Organochlorine Pesticides (OCPs) from East Asia to the Arctic Ocean

Hongyuan Zheng[1,2,3], Yuan Gao[1], Yinyue Xia[1], Haizhen Yang[2,3], and Minghong Cai[1]

[1]Ministry of Natural Resources Key Laboratory for Polar Sciences, Polar Research Institute of China, 451 Jinqiao Road, Shanghai 200136, China

[2]College of Environmental Science and Engineering, Tongji University, 1239 Siping Road, Shanghai 200092, China

[3]State Key Laboratory of Pollution Control and Resource Reuse, Tongji University, 1239 Siping Road, Shanghai 200092, China

Correspondence to: M.-H, Cai,

Tel.: +86-21-58717635; fax: +86-21-58711663

E-mail: caiminghong@pric.org.cn

Number of pages: 15 (including cover page);

Number of figures: 9;

List of Contents:

Figure S1 The sampling stations of the surface seawater and atmosphere from East Asia to the high Arctic Ocean during the 7th Chinese National Arctic Research Expedition (2016):

a. Forward Cruise sampling station of surface seawater from July to August (**A1-26**);

b. Backward Cruise sampling station of surface seawater from late Agust to September (**A27-74**);

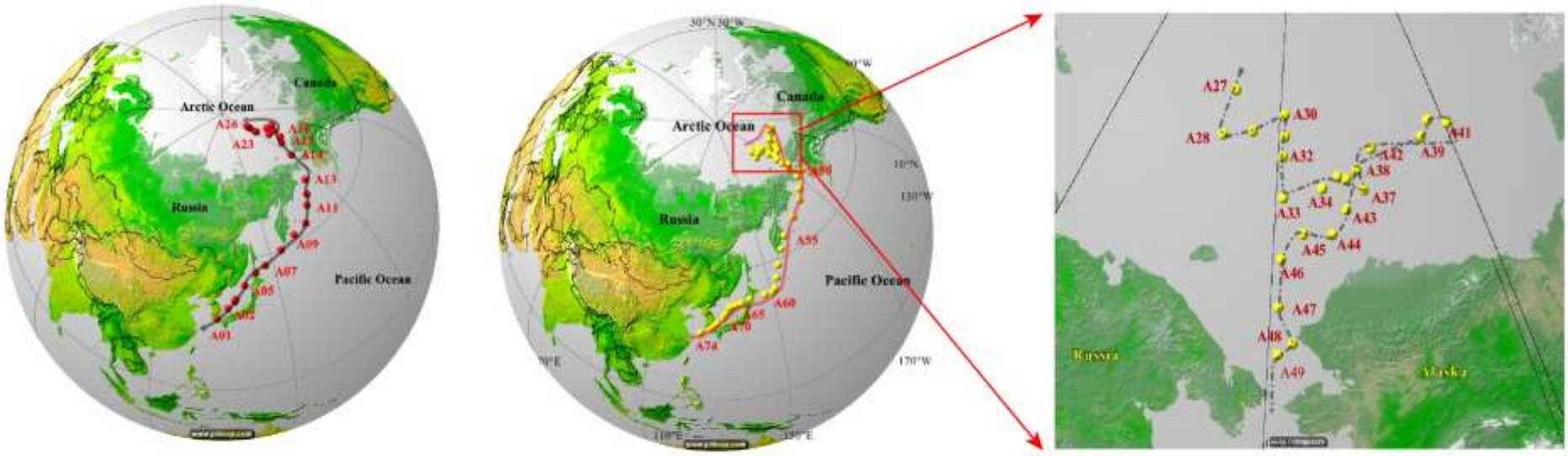

(a) (b)

Figure S2 The sampling stations of the surface seawater and atmosphere from the high Arctic Ocean to East Asia during the 8th Chinese National Arctic Research Expedition (2017):

a. Sampling station of surface seawater (**B1-16**);

b. Sampling station of the atmosphere (**C1-16**): C1-9 Forward Cruise sampling station (△), C10-16 Backward Cruise sampling station (○)

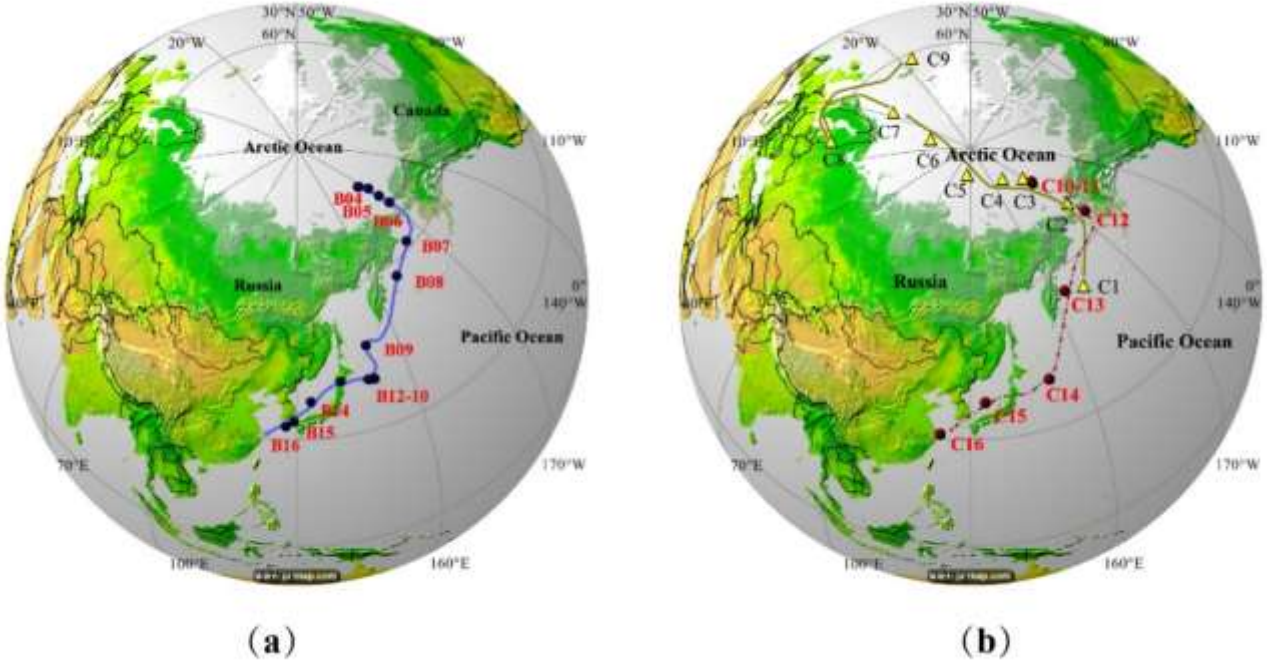

Figure S3 Schematic diagrams of the High-volume Solid-phase Extraction system

(A) the high-volume solid-phase extraction water sampler;

(B) the high-volume solid-phase extraction atmospheric sampler,

(C) In situ internal ultrasonic treatment (ISIU) and structure diagram of the high-volume solid-phase adsorption column for both water and atmosphere.

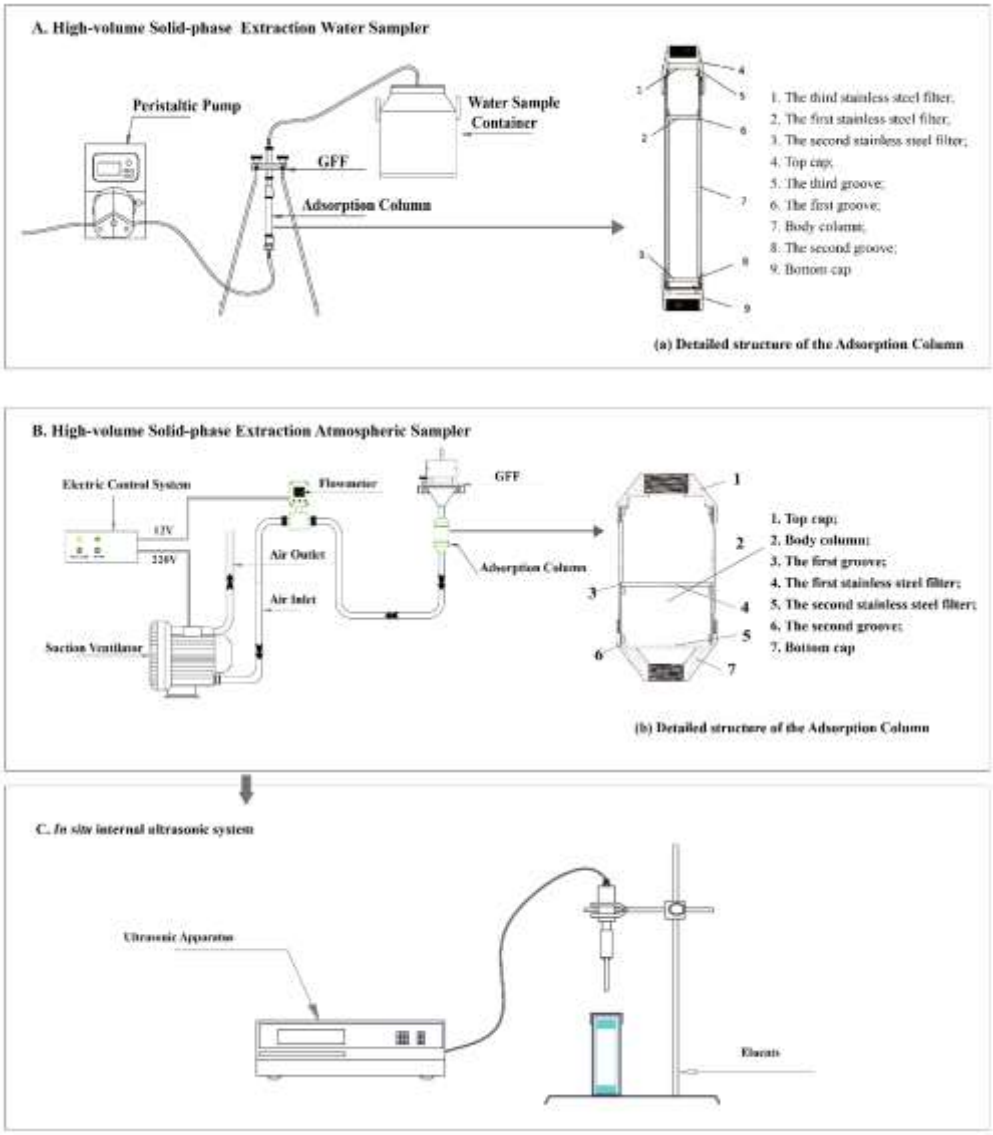

Figure S4 The position of the High-volume Solid-phase Extraction water and atmospheric samplers, automatic surface seawater acquisition system fixedly mounted on the Chinese Research Vessel Xuelong (Snow Dragon).

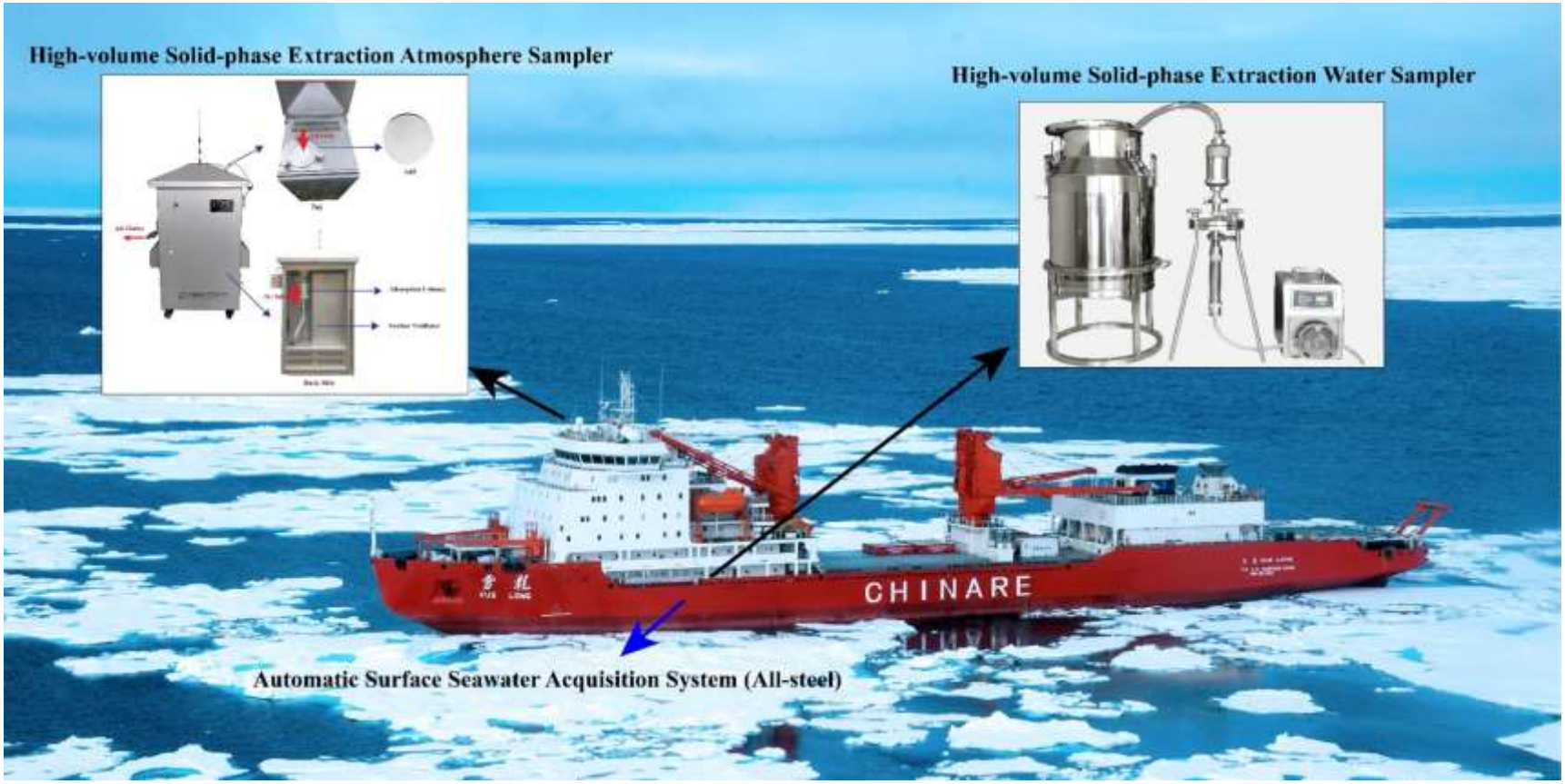

Figure S5 The box plot of the individual HCH and DDT from the samples from East Asia to the high Arctic

a. Forward voyage (surface seawater, A01-26) during the 7th Chinese National Arctic Research Expedition (2016);

b. Return voyage (surface seawater, A27-74) during the 7th Chinese National Arctic Research Expedition (2016).;

c. Return Voyage (surface seawater, B01-16) during the 8th Chinese National Arctic Research Expedition (2017);

d. Forward voyage (atmosphere, C01-09) during the 8th Chinese National Arctic Research Expedition (2017);

e. Return Voyage (atmosphere, C10-16) during the 8th Chinese National Arctic Research Expedition (2017).

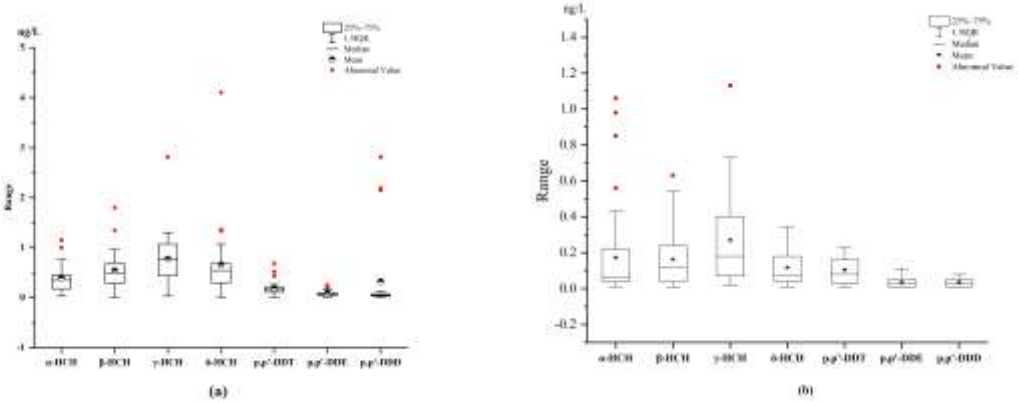

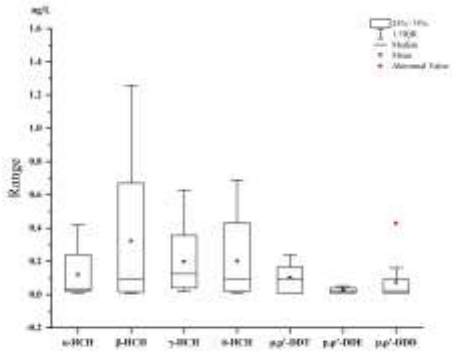
Range
α-HCH
β-HCH
γ-HCH
δ-HCH
p,p'-DDT
p,p'-DDE
p,p'-DDD

(c)

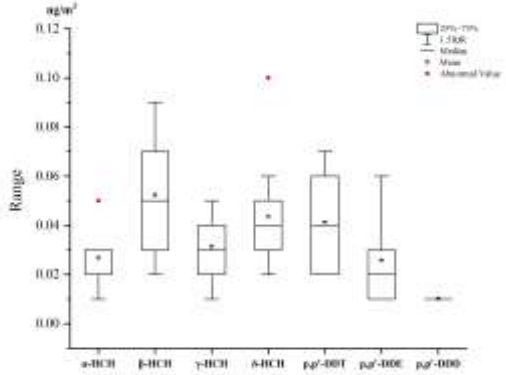
ng/m³
Range
α-HCH
β-HCH
γ-HCH
δ-HCH
p,p'-DDT
p,p'-DDE
p,p'-DDD

(d)

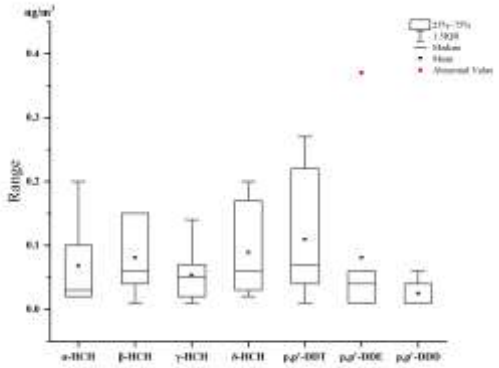
ng/m³
Range
α-HCH
β-HCH
γ-HCH
δ-HCH
p,p'-DDT
p,p'-DDE
p,p'-DDD

(e)

Figure S6 The air-mass back trajectories of the atmosphere samples (C01-16)

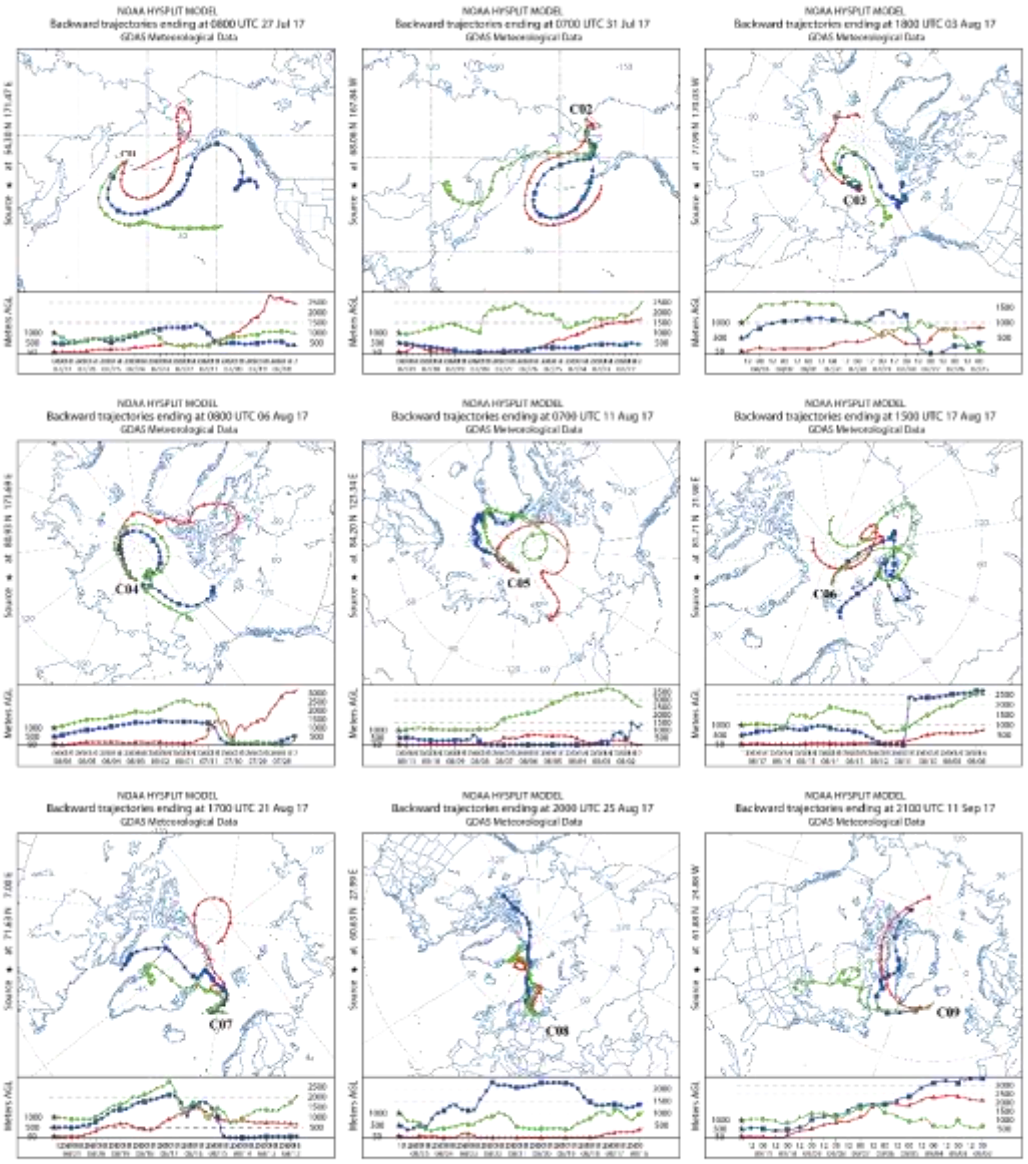

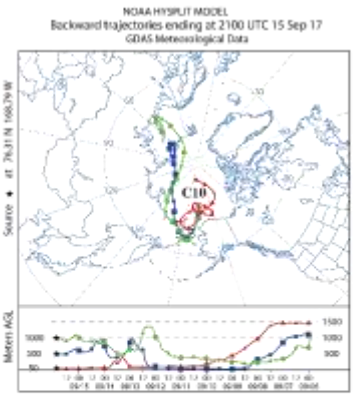
NOAA HYSPLIT MODEL
Backward trajectories ending at 2100 UTC 15 Sep 17
GDAS Meteorological Data
C10

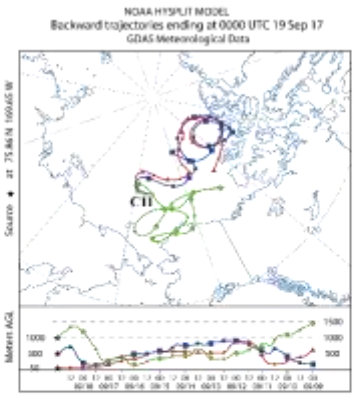
NOAA HYSPLIT MODEL
Backward trajectories ending at 0000 UTC 19 Sep 17
GDAS Meteorological Data
C11

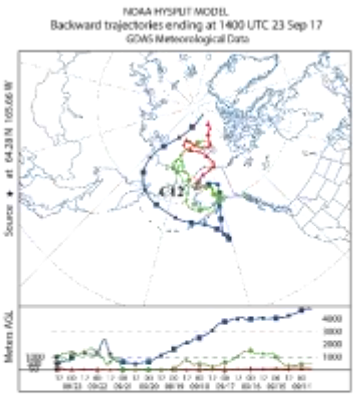
NOAA HYSPLIT MODEL
Backward trajectories ending at 1400 UTC 23 Sep 17
GDAS Meteorological Data
C12

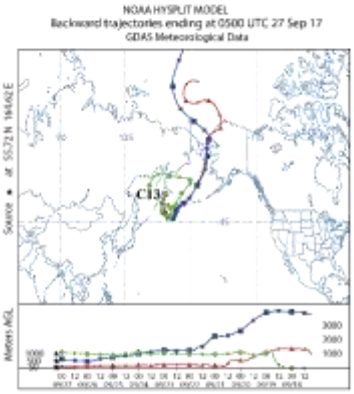
NOAA HYSPLIT MODEL
Backward trajectories ending at 0500 UTC 27 Sep 17
GDAS Meteorological Data
C13

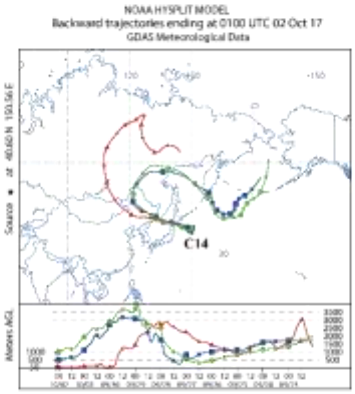
NOAA HYSPLIT MODEL
Backward trajectories ending at 0100 UTC 02 Oct 17
GDAS Meteorological Data
C14

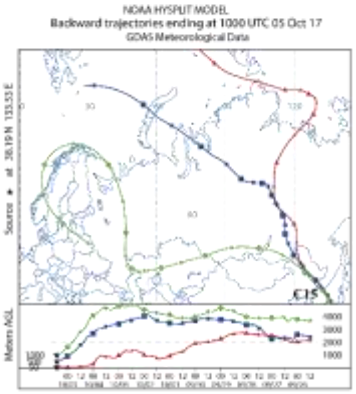
NOAA HYSPLIT MODEL
Backward trajectories ending at 1000 UTC 05 Oct 17
GDAS Meteorological Data
C15

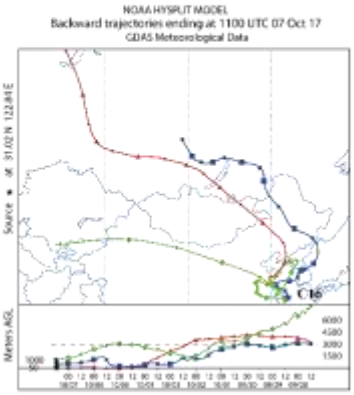
NOAA HYSPLIT MODEL
Backward trajectories ending at 1100 UTC 07 Oct 17
GDAS Meteorological Data
C16

Figure S7 The demarcation map of the source regions for the atmosphere samples in the North Hemisphere

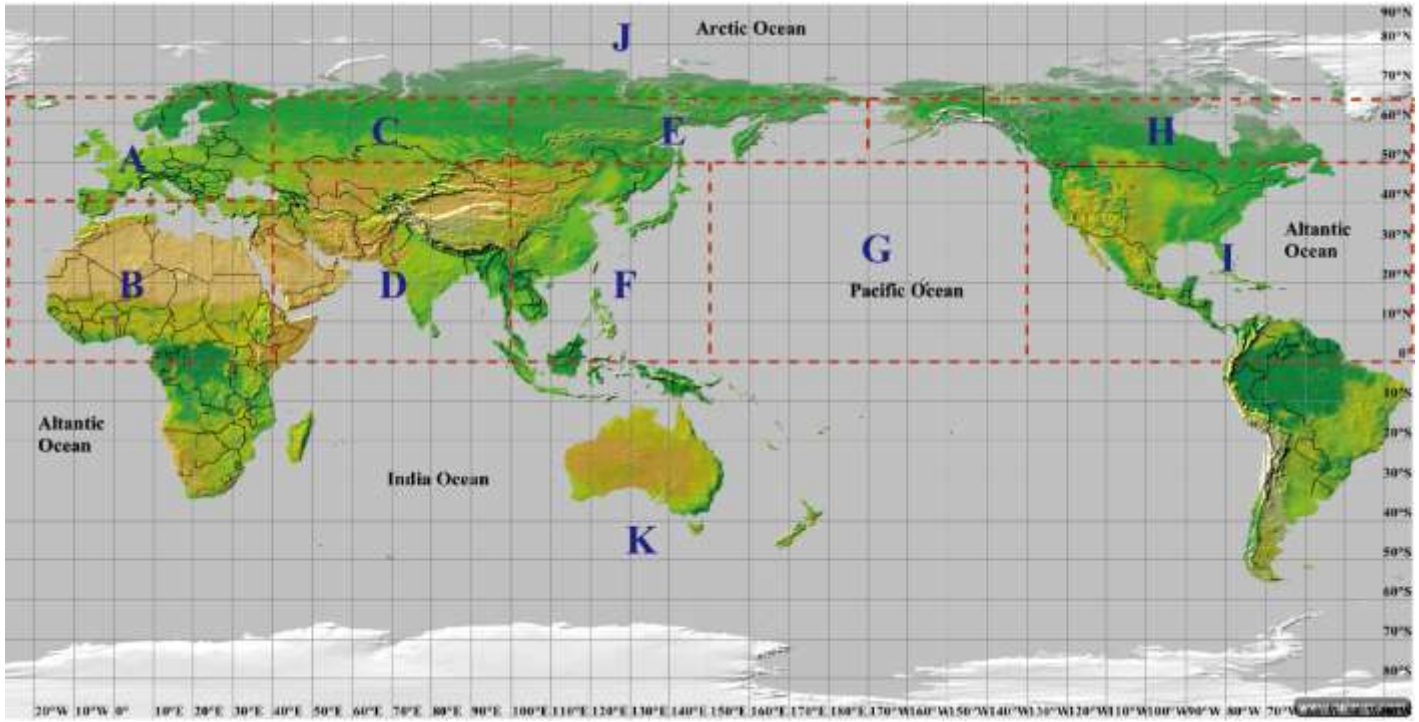

Annotation

A: Europe 40°N-66.57°N, 30°W-40°E ; B: North Africa 0°N-40°N,30°W-40°E; C:West Russia 50°N-66.57°N,40°E-100°E; D: Middle East-West Asia 0°N-50°N,40°E-100°E; E: East Russia and Coast Regions 50°N-66.57°N,100°E-170°W; F:East Asia 0°N-50°N,100°E-150°E; G: North Pacific Ocean 0°N-50°N, 150°E-130°W; H Canada and Alaska50°N-66.57°N, 170°W-30°W; I: The USA and middle Latin America 0°N-50°N,130°W-30°W; J: Arctic 66.57°N-90°N, 30°W-30°W; K:South Hemisphere 0°S-90°S, 30°W-30°W.

Figure S8 The sea ice extent in the Northern Hemisphere during the sampling period in 2016 and 2017

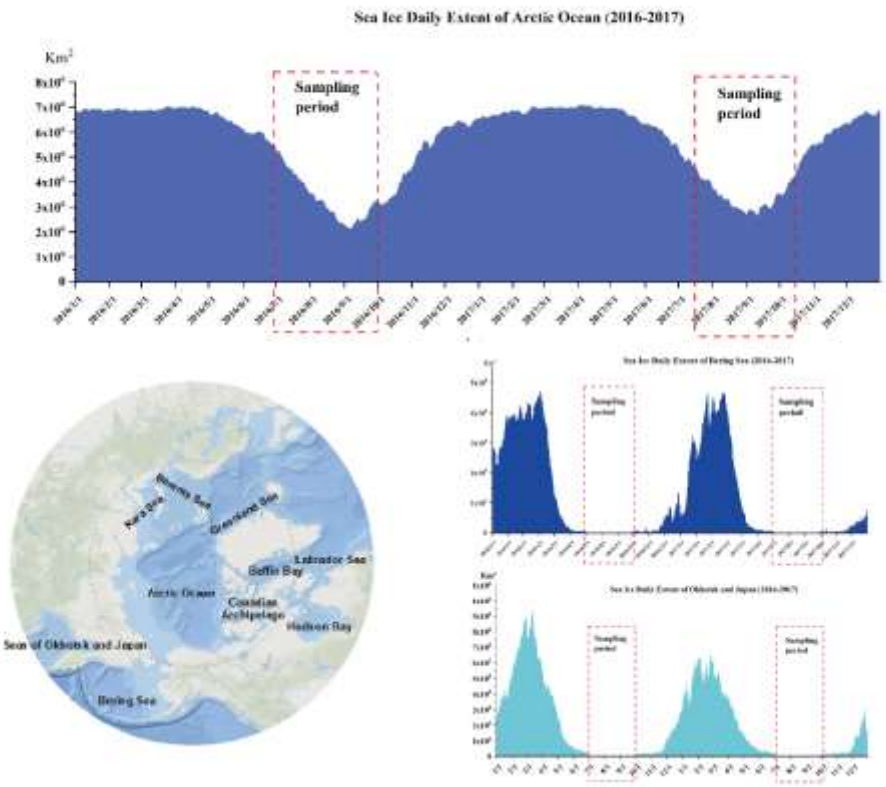

Annotation:
Data originated from the National Snow and Ice Data Center https://nsidc.org/data/

Figure S9 The diffusion map of individual HCH, DDT, salinity, and temperature in the surface seawater of the East Arctic Ocean (A14-49) in 2016.

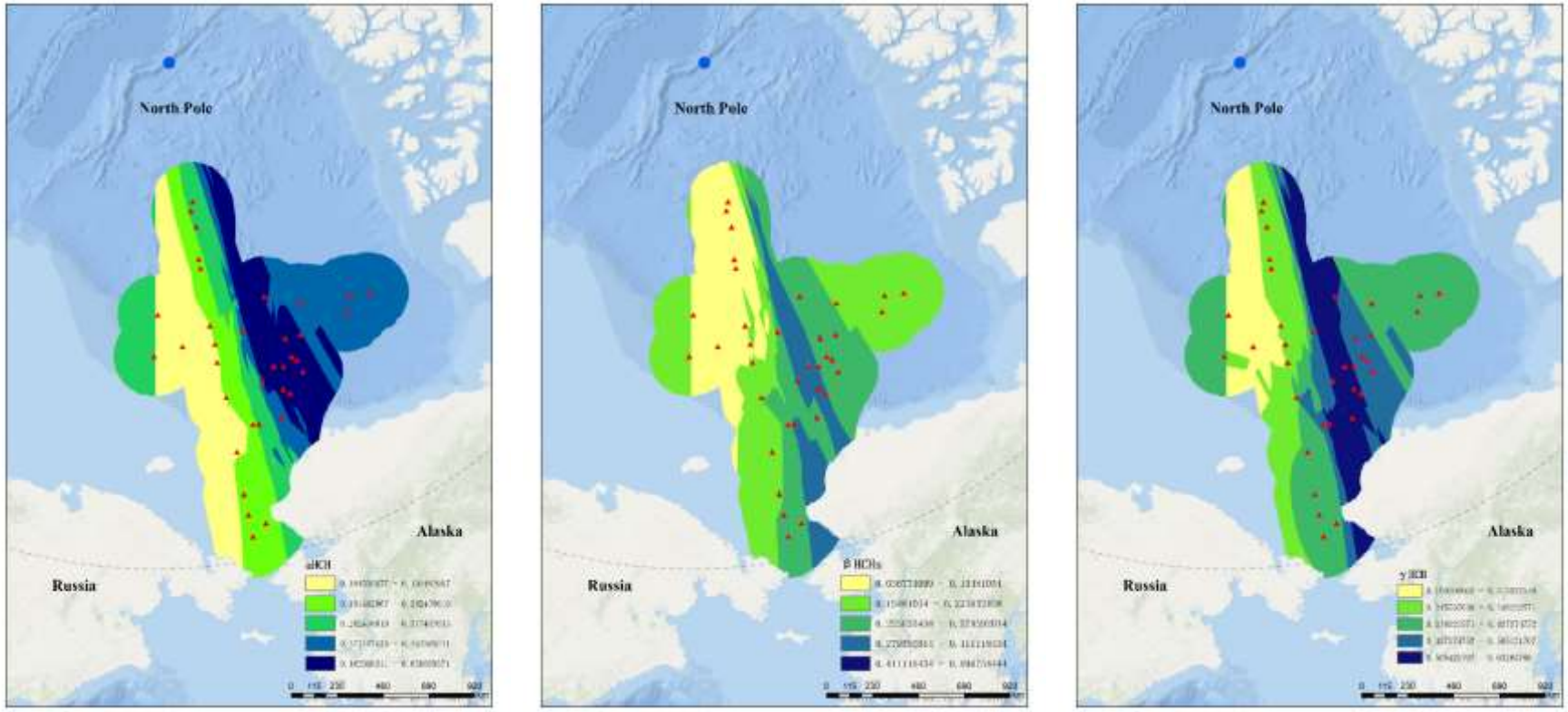

α-HCH β-HCH γ-HCH

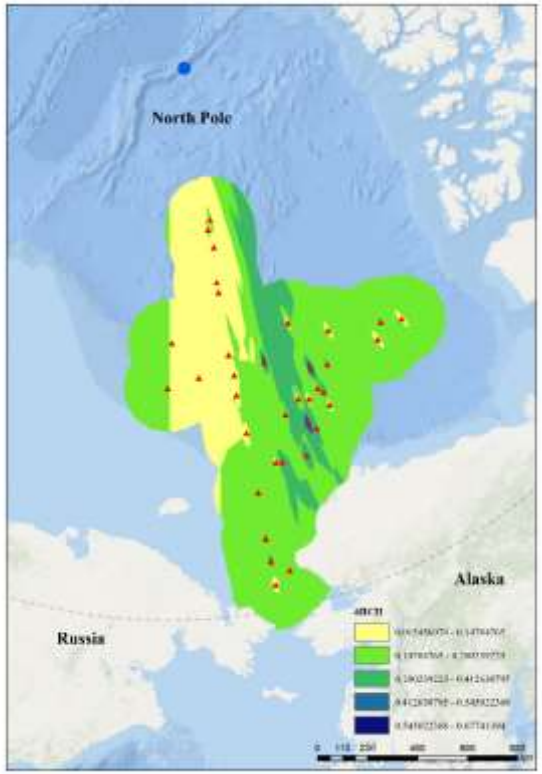

δ-HCH

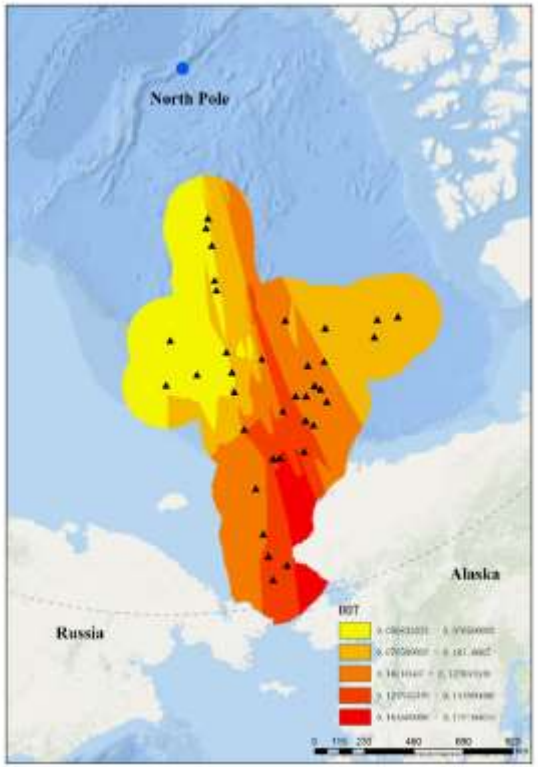

p,p'-DDT

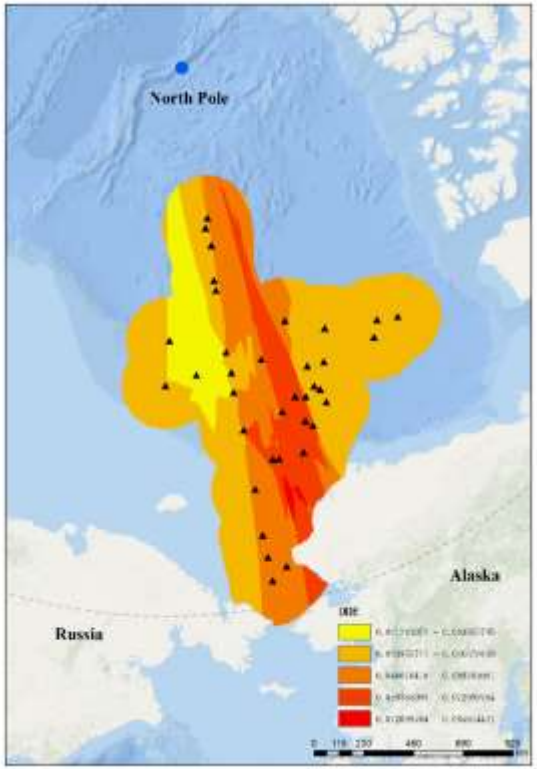

p,p'-DDE

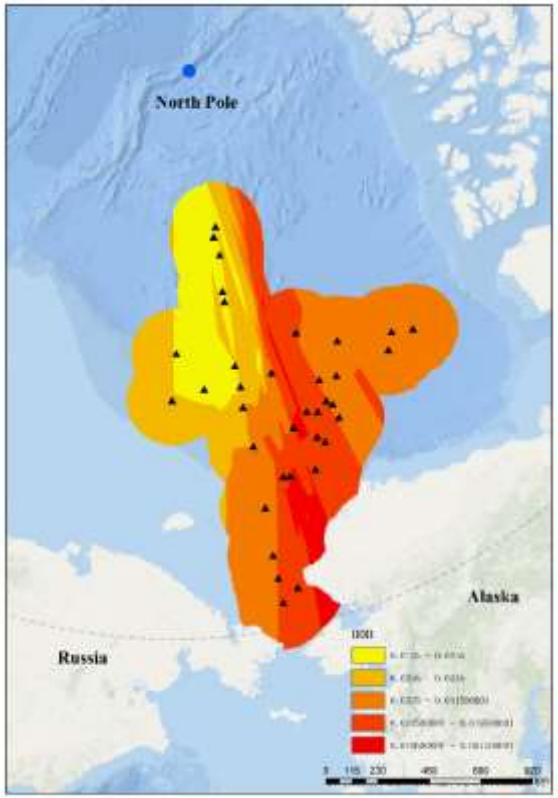

p,p'-DDD

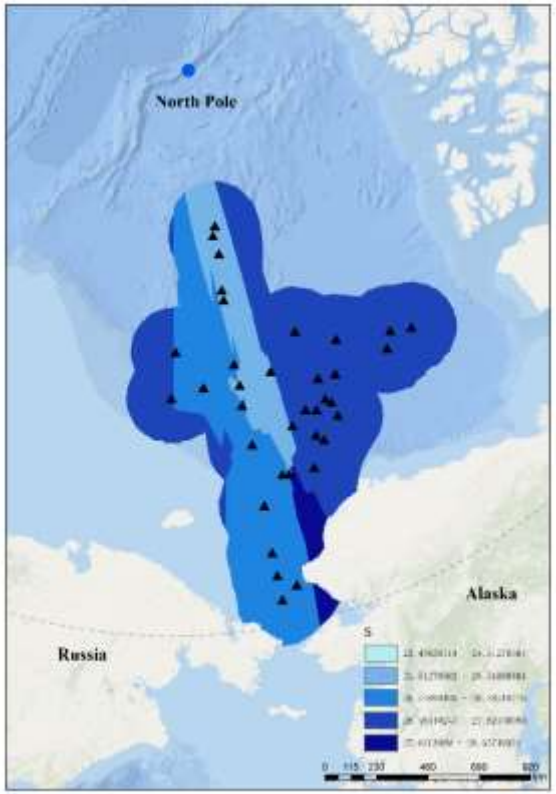

Salinity

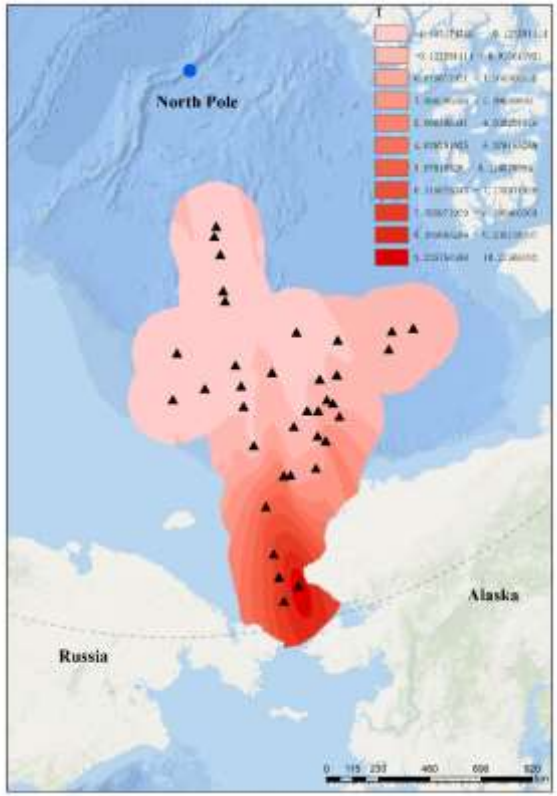

Temperature